

Boise State University

ScholarWorks

Geosciences Faculty Publications and
Presentations

Department of Geosciences

8-1-2019

Examining the Tectono-Stratigraphic Architecture, Structural Geometry, and Kinematic Evolution of the Himalayan Fold-Thrust Belt, Kumaun, Northwest India

Subhadip Mandal
University of Alabama

Delores M. Robinson
University of Alabama

Matthew J. Kohn
Boise State University

Subodha Khanal
Georgia Department of Transportation

Oindrila Das
University of Alabama

—

Examining the tectono-stratigraphic architecture, structural geometry, and kinematic evolution of the Himalayan fold-thrust belt, Kumaun, northwest India

Subhadip Mandal^{1,*}, Delores M. Robinson¹, Matthew J. Kohn², Subodha Khana³, and Oindrila Das¹

¹DEPARTMENT OF GEOLOGICAL SCIENCES, CENTER FOR SEDIMENTARY BASIN STUDIES, UNIVERSITY OF ALABAMA, BEVILL BUILDING, TUSCALOOSA, ALABAMA 35487, USA

²DEPARTMENT OF GEOSCIENCES, BOISE STATE UNIVERSITY, 1910 UNIVERSITY DRIVE, BOISE, IDAHO 83725, USA

³GEORGIA DEPARTMENT OF TRANSPORTATION, 600 WEST PEACHTREE STREET NORTHWEST, ATLANTA, GEORGIA 30308, USA

ABSTRACT

Existing structural models of the Himalayan fold-thrust belt in Kumaun, northwest India, are based on a tectono-stratigraphy that assigns different stratigraphy to the Ramgarh, Berinag, Askot, and Muniari thrusts and treats the thrusts as separate structures. We reassess the tectono-stratigraphy of Kumaun, based on new and existing U-Pb zircon ages and whole-rock Nd isotopic values, and present a new structural model and deformation history through kinematic analysis using a balanced cross section. This study reveals that the rocks that currently crop out as the Ramgarh, Berinag, Askot, and Muniari thrust sheets were part of the same, once laterally continuous stratigraphic unit, consisting of Lesser Himalayan Paleoproterozoic granitoids (ca. 1850 Ma) and metasedimentary rocks. These Paleoproterozoic rocks were shortened and duplexed into the Ramgarh-Muniari thrust sheet and other Paleoproterozoic thrust sheets during Himalayan orogenesis. Our structural model contains a hinterland-dipping duplex that accommodates ~541–575 km or 79%–80% of minimum shortening between the Main Frontal thrust and South Tibetan Detachment system. By adding in minimum shortening from the Tethyan Himalaya, we estimate a total minimum shortening of ~674–751 km in the Himalayan fold-thrust belt. The Ramgarh-Muniari thrust sheet and the Lesser Himalayan duplex are breached by erosion, separating the Paleoproterozoic Lesser Himalayan rocks of the Ramgarh-Muniari thrust into the isolated, synclinal Almora, Askot, and Chiplakot klippen, where folding of the Ramgarh-Muniari thrust sheet by the Lesser Himalayan duplex controls preservation of these klippen. The Ramgarh-Muniari thrust carries the Paleoproterozoic Lesser Himalayan rocks ~120 km southward from the footwall of the Main Central thrust and exposed them in the hanging wall of the Main Boundary thrust. Our kinematic model demonstrates that propagation of the thrust belt occurred from north to south with minor out-of-sequence thrusting and is consistent with a critical taper model for growth of the Himalayan thrust belt, following emplacement of midcrustal Greater Himalayan rocks. Our revised stratigraphy-based balanced cross section contains ~120–200 km greater shortening than previously estimated through the Greater, Lesser, and Subhimalayan rocks.

LITHOSPHERE, v. 11; no. 4; p. 414–435; GSA Data Repository Item 2019153 | Published online 25 April 2019

<https://doi.org/10.1130/L1050.1>

INTRODUCTION

Beginning ca. 60–55 Ma (Najman et al., 2010; DeCelles et al., 2016), continental collision between the Indian and Asian plates created the Himalayan-Tibetan orogenic system, consisting of the Tibetan Plateau and the Himalayan fold-thrust belt, an ~2500-km-long, arcuate belt, primarily consisting of north-dipping and folded thrusts of upper- and midcrustal rocks lying south of the Indus-Tsangpo suture (Fig. 1A; for reviews, see Yin and Harrison, 2000; Yin, 2006). This fold-thrust belt has been used to study large-scale tectonic processes, for example, (1) processes in the Himalaya that are spatially and temporally linked to the growth of the Tibetan Plateau (e.g., DeCelles et al., 2002; Robinson et al., 2006; Long et al., 2011; Yu et al., 2015; Webb et al., 2017; and references therein), (2) continent-continent collision dynamics governing mountain building processes and metamorphism (e.g., Bollinger et al., 2006; Jamieson

and Beaumont, 2013; Kohn, 2014; Avouac 2015; and references therein), (3) interplay between climate and tectonics (e.g., Clift, 2006; and references therein), (4) kinematics and mechanics of upper-crustal deformation (e.g., Webb, 2013; Robinson and Martin, 2014; Bhattacharyya et al., 2015a; and references therein), and (5) structures that are potential seismotectonic hazards (e.g., Elliott et al., 2016; Grandin et al., 2016; Searle et al., 2016). While these studies have dramatically improved our understanding of orogenic dynamics, multiple models compete to explain the evolution of the Himalayan system, including: channel flow (Beaumont et al., 2001, 2004), extrusion (Burchfiel and Royden, 1985; Grujic et al., 1996), tectonic wedging (Yin, 2006; Webb et al., 2007; He et al., 2015, 2016), and critical taper (Avouac, 2003; Bollinger et al., 2006; Robinson et al., 2006; Kohn, 2008, 2014; Long et al., 2011). However, channel flow and critical taper, instead of being mutually exclusive, may be spatially and temporally linked through two or more stages of growth of the Himalaya (Beaumont and Jamieson, 2010; Wang et al., 2015; Cottle et al., 2015, references therein; Parsons et al., 2016). For example, brief channel flow, involving extrusion and exhumation of Greater Himalayan migmatites as

*Corresponding author: smandal@crimson.ua.edu. Present address: Core Laboratories, 6323 Windfern Road, Houston, Texas 77040, USA.

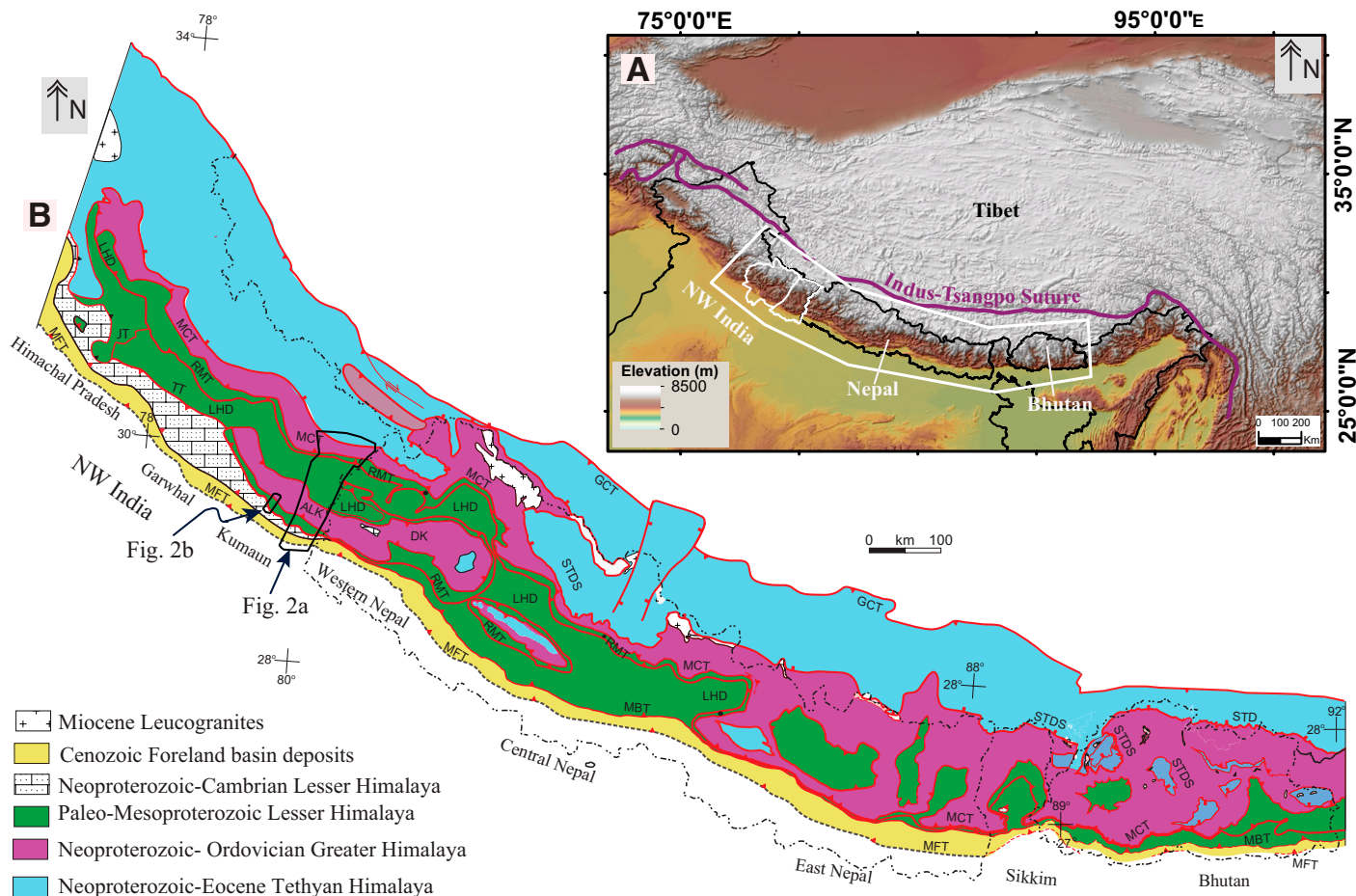


Figure 1. (A) Digital elevation model (using Advanced Spaceborne Thermal Emission and Reflection Radiometer [ASTER] global digital elevation data set) of the Himalayan-Tibetan orogenic system. Purple line is the Indus-Tsangpo suture zone (modified after C  lerier et al., 2009). White box outlines the location of part B. The two white outlined regions in NW India are Garhwal to the west and Kumaun to the east. (B) Generalized tectono-stratigraphic map of northwest India, Nepal, Sikkim, and Bhutan (modified from Robinson and Pearson, 2013). ALK—Almora klippe; DK—Dadeldhura klippe; GCT—Great Counter thrust; JT—Jutogh thrust; LHD—Lesser Himalayan duplex; MBT—Main Boundary thrust; MCT—Main Central thrust; MFT—Main Frontal thrust; RMT—Ramgarh-Munsiari thrust; STDS—South Tibetan Detachment system; TT—Tons thrust. Dadeldhura klippe is the eastern continuation of the Almora klippe, often referred to as Almora-Dadeldhura klippe.

a weak midcrustal channel in early Miocene time (ca. 20 Ma), may have been bracketed or succeeded (<17 Ma) by critical taper dynamics (foreland fold-thrust belt) involving in-sequence thrusting and exhumation of Lesser Himalayan rocks and/or cooled Greater Himalayan rocks (Beaumont and Jamieson, 2010; Wang et al., 2015, and references therein). Thus, to understand the development of the Himalayan fold-thrust belt from the early Miocene to the present, the kinematic evolution of the Lesser Himalayan and Subhimalayan rocks (Fig. 1B), south of the metamorphic core, must be investigated. However, poor chrono- and tectono-stratigraphic knowledge of the Lesser Himalayan rocks has led to erroneous assumptions about the structural geometries, therefore preventing accurate quantification of along-strike variations in structural geometry, kinematics, and shortening magnitudes (e.g., Yu et al., 2015).

Lesser Himalayan rocks are stacked in a series of in-sequence, south-vergent, predominantly north-dipping to antiformal thrust sheets, forming the Lesser Himalayan duplex; this duplex accommodates a significant proportion of total Lesser Himalayan shortening (Srivastava and Mitra, 1994; DeCelles et al., 2001; Robinson et al., 2003, 2006; McQuarrie et al., 2008; Long et al., 2011; Bhattacharyya et al., 2015a; Parui and Bhattacharyya, 2018). This duplex is nonuniformly expressed and exposed

along the Himalayan arc, with variations in structural geometries and magnitudes of minimum shortening. In northwest India and Nepal, the Lesser Himalayan duplex is hinterland-dipping (Robinson et al., 2006; Khanal and Robinson, 2013; Webb, 2013; Yu et al., 2015), antiformally stacked in Sikkim (Bhattacharyya and Mitra, 2009; Bhattacharyya et al., 2015a; Parui and Bhattacharyya, 2018), and hinterland-dipping in Bhutan and Arunachal (Yin et al., 2010; Long et al., 2011; DeCelles et al., 2016). Progressive growth of this duplex caused passive folding of the overlying Greater and Tethyan Himalayan rocks to expose the Himalayan metamorphic core (Srivastava and Mitra, 1994; DeCelles et al., 2001; Robinson et al., 2003; Mitra et al., 2010). Therefore, understanding the growth and kinematic evolution of the Lesser Himalayan duplex and its resultant displacement-transfer of roof thrust(s) is pivotal to unraveling the growth of the fold-thrust belt, and helping to determine the way in which convergence between India and Asia was accommodated (van Hinsenberg et al., 2012; Li et al., 2015).

Kumaun lies in a zone of nearly normal convergence at high convergence rates, so this area should record a high magnitude of upper-crustal shortening. Our knowledge of the structural/geometrical architecture and evolution of Kumaun comes from previous work by Valdiya (1980)

and Srivastava and Mitra (1994). However, as we show here, incorrect correlation of stratigraphy among various thrust sheets that locally occur as synformal klippen invalidates the structural model and shortening estimates of Srivastava and Mitra (1994). Receiver function seismic data provide an additional constraint on the location of the Lesser Himalayan midcrustal ramp in the Main Himalayan thrust (Caldwell et al., 2013). Here, we present evidence for new stratigraphic correlations and a new structural model that illustrates the geometry of the Himalayan fold-thrust belt in Kumaun. First, we reassess the tectono-stratigraphy through a combination of new and existing field, U-Pb zircon, and whole-rock Nd isotopic data. Then, with this refined tectono-stratigraphy and new location of the crustal ramp geometry (Caldwell et al., 2013), we construct a balanced cross section and a sequential kinematic model, and we estimate shortening.

TECTONO-STRATIGRAPHY

The Himalayan fold-thrust belt (Fig. 1B) is composed of Greater Indian pre-Cenozoic northern margin rocks that were deposited over the ca. 2500 Ma Indian cratonic basement and scraped off during collision between India and Asia (see McQuarrie et al., 2008). The resulting fold-thrust belt is divided into four tectono-stratigraphic zones (Heim and Gansser, 1939; Gansser, 1964), which are, from north to south, the Tethyan Himalaya, Greater Himalaya (synonymous with High Himalayan Crystalline Series), Lesser Himalaya, and Subhimalaya (Fig. 1B). Each of these tectono-stratigraphic zones has a distinctive stratigraphy and metamorphic grade and is separated from adjacent zones by major crustal-scale faults. The South Tibetan Detachment system separates the Tethyan Himalayan rocks from the Greater Himalayan rocks (Burchfiel et al., 1992). The Main Central thrust/Vaikrita thrust separates the Greater Himalayan rocks from the Lesser Himalayan rocks; this definition follows the original structural analysis of Heim and Gansser (1939). The Ramgarh, Munsiri, and Berinag thrusts and Lesser Himalayan duplex are intra-Lesser Himalayan faults that juxtapose panels of Lesser Himalayan rocks (Figs. 2A and 2B). The Main Boundary thrust separates Lesser Himalayan from Subhimalayan rocks. The Main Frontal thrust separates the Subhimalayan rocks from the Indo-Gangetic plain alluvium. At depth, these faults sole into the Main Himalayan thrust, which is the basal décollement. In the next sections, we briefly review the tectono-stratigraphy, including new (this study) and existing field data (Rupke 1974; Valdiya, 1980; Srivastava and Mitra, 1994; Célérier et al., 2009; McKenzie et al., 2011; Mandal et al., 2015, 2016). Rock unit names and brief descriptions of lithology are listed in Table 1.

Subhimalaya

In Kumaun, Subhimalayan rocks (Fig. 2A; Table 1) are composed of coarsening-upward, Neogene sedimentary rocks (~6.0 km thick; Najman, 2006; Jain et al., 2009; Ravikant et al., 2011) that were shed from the adjacent growing Himalayan thrust belt (Praksh et al., 1980; DeCelles et al., 1998; Kumar et al., 2004; Najman et al., 2008). Within the Subhimalayan zone, the Siwalik Group is informally divided into lower, middle, and upper units (Harrison et al., 1993; DeCelles et al., 1998, 2001, 2002). The lower Siwalik unit (Fig. 3A), deposited between 13 and 11 Ma (White et al., 2002; Kumar et al., 2004; Ravikant et al., 2011), is an ~1500-m-thick (Fig. 2A) succession of alternating sandstone and mudstone. The middle Siwalik unit, deposited between 11 and 4.5 Ma (Kumar et al., 2004), is a >2300-m-thick, vertically and laterally stacked sandstone complex. The upper Siwalik unit, deposited between 4.5 and 1 Ma (Kumar et al., 2004), is an ~2300-m-thick succession of bedded conglomerate with lenticular bodies of sandstone and rare mudstone. The upper Siwalik unit is not

exposed in this study area, so we used the nearest exposed upper Siwalik unit, ~80 km west of the study area, for the thickness (Raiverman, 2002). Pre-Siwalik Group foreland basin units (e.g., Subathu/Bhainskati, Dagshai-Kasauli/Dumri Formations) crop out intermittently in the hanging wall and footwall of the Main Boundary thrust (Mukhopadhyay and Mishra, 2005; Robinson et al., 2006; Mishra and Mukhopadhyay, 2012). In eastern Kumaun, the lower Siwalik unit, as well as Neogene pre-Siwalik foreland basin strata (Lugad Gad Formation; Fig. 3B; Rupke, 1974), crop out between the Main Frontal thrust and Main Boundary thrust (Fig. 2A; Table 1) in the Subhimalayan thrust system as three thrust sheets: the Main Frontal thrust sheet, an unnamed sheet, and the Main Dun thrust sheet. The Main Frontal thrust sheet is ~2900 m thick and contains a mudstone-sandstone sequence, including paleosols, of the lower Siwalik unit and the thickly bedded gray sandstone of the middle Siwalik unit. The basal part of the overlying Main Dun thrust sheet contains ~300 m of pale-green, biotite-rich sandstone of the Lugad Gad Formation (Rupke, 1974; Karunakaran and Rao, 1979), which is equivalent to the early Miocene Dumri Formation of western Nepal and Kasauli/upper Dharamsala Formation of Himachal Pradesh (Najman, 2006). Lugad Gad sandstone has prolific paleosol horizons, ripples, and high biotite content, which are nearly absent in the overlying Siwalik sandstone. The Lugad Gad Formation is overlain by mudstone-dominated lower Siwalik Group rocks in the Main Dun thrust sheet (Figs. 2A and 3A).

Lesser Himalaya

In India, the Lesser Himalayan sequence is composed of Paleoproterozoic to Cambrian igneous and metasedimentary rocks and is divided into two parts, Paleoproterozoic–Mesoproterozoic Lesser Himalayan rocks (1900–1600 Ma) and Neoproterozoic Lesser Himalayan rocks (1100–500 Ma), commonly referred as lower Lesser Himalaya and upper Lesser Himalaya, respectively (McKenzie et al., 2011; Mandal et al., 2016). Detailed descriptions of Lesser Himalayan rocks have been presented elsewhere (Valdiya, 1980; Srivastava and Mitra, 1994; Célérier et al., 2009; Patel et al., 2007, 2011; Mandal et al., 2015) and are summarized in Table 1. Paleoproterozoic–Mesoproterozoic Lesser Himalayan rocks include the Berinag–Munsiri and Rautgara Formations (Figs. 3C–3D), while Neoproterozoic–Cambrian Lesser Himalayan rocks include the Mandhali, Chandpur, Nagthat, Blaini, and Krol Formations (Figs. 2A and 2B; Table 1). The age of the Deoban Formation (Fig. 3E) is controversial, and proposed ages have ranged from latest Paleoproterozoic to latest Neoproterozoic (see discussion in Mandal et al., 2015). Because of lithologic similarity, and potentially overlapping ages, we group it with the Mandhali Formation (Fig. 3F). Basal Paleoproterozoic–Mesoproterozoic Lesser Himalayan rocks (i.e., greenschist- to lower-amphibolite-facies Berinag–Munsiri Formation[s]) often crop out within the Lesser Himalayan tectono-stratigraphic zone as synclinal klippen, known as Lesser Himalayan Crystalline nappes/klippen (Fig. 4A) (e.g., Askot and Chiplakot klippen). Paleoproterozoic–Mesoproterozoic Lesser Himalayan rocks have very negative whole-rock neodymium isotopic values ($\epsilon_{Nd} = \sim -24.0$; Ahmad et al., 2000; Robinson et al., 2001; Martin et al., 2005; Richards et al., 2005; Mandal et al., 2015; Martin, 2017), while Neoproterozoic–Cambrian Lesser Himalayan and Greater Himalayan rocks have less negative ϵ_{Nd} values (~ -15.0 ; Ahmad et al., 2000; Robinson et al., 2001; Richards et al., 2005). Neoproterozoic–Cambrian Lesser, Greater, and Tethyan Himalayan rocks are difficult to distinguish using depositional ages and ϵ_{Nd} values alone, because they may have been part of a single Neoproterozoic continental margin (Myrow et al., 2003, 2015; McKenzie et al., 2011). An estimated Lesser Himalayan minimum thickness is 8.7–10.9 km in far western Nepal (Robinson et al., 2006), whereas in Kumaun, we use

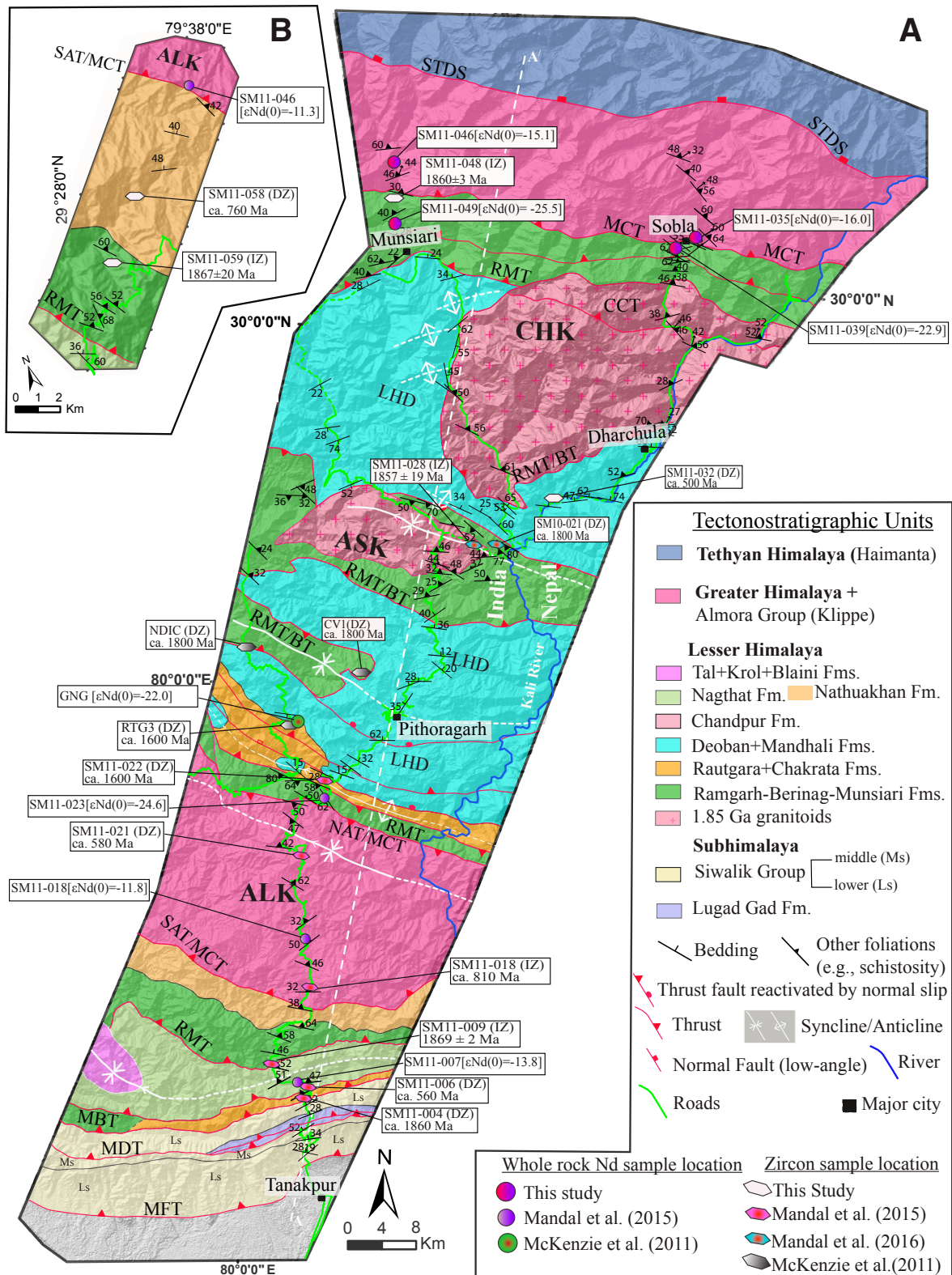


Figure 2. (A) Geologic map of Kumaun, India, with the cross-section line A–A' shown as a white dashed line and sample locations. (B) Geological map of the southern margin of the Almora klippe, east of the region in A, showing continuity of stratigraphy and locations of two zircon samples discussed in the text. For sample identifications, IZ—igneous zircon sample; DZ—detrital zircon sample. ALK—Almora klippe, ASK—Askot klippe, CHK—Chiplakot klippe; BT—Berinig thrust; CCT—Central Chiplatek thrust, LHD—Lesser Himalayan duplex; MBT—Main Boundary thrust; MCT—Main Central thrust; MDT—Main Dun thrust; MFT—Main Frontal thrust; NAT—North Almora thrust; RMT—Ramgarh-Munsiari thrust; SAT—South Almora thrust; STDS—South Tibetan Detachment system.

TABLE 1. GENERALIZED TECTONO-STRATIGRAPHY OF KUMAUN, INDIA, WITH THICKNESS ORGANIZED FROM NORTH (TOP) TO SOUTH (BOTTOM) ALONG THE CROSS-SECTION LINE

	Unit Name	Lithology	Thickness (m)
Tethyan Himalaya	Martoli Formation/Budhi Schist (Haimanta equivalent)	Phyllite, mica schist, calcareous schist, and pegmatites (Valdiya et al., 1999; Patel et al., 2011)	~6500
	STDS		
Greater Himalaya	Badrinath/Pindari Formation Pandukeshwar Formation Joshimath Formation 	Sillimanite-bearing augen gneiss Micaceous-quartzite Kyanite-bearing gneiss (Spencer et al., 2012a)	10500
	Vaikrita Group		
Lesser Himalaya	Munsiri Formation [ca. 1800 Ma] [1860 ± 3 Ma granitoid gneiss] 	Garnet mica schist, calc-silicate, quartzite, and granitoid-gneiss	~7000
	Berinag Formation [ca. 1800 Ma] 	Sericitic quartzite, schistose quartzite, garnet-schist, granitoid gneiss, and mafic sill	900
	Mandhali Formation [<950 Ma] Gangolihat Formation Rautgara Formation [ca. 1600 Ma] 	Carbonaceous phyllite, slate, and minor limestone Stromatolite-bearing cherty dolomite and dolomitic limestone Argillaceous quartzite, phyllite, and mafic sill	5250
Greater Himalaya	Almora (Champawat) Granitoids [ca. 500 Ma] Saryu-Gumalikhet Formation [800-580 Ma] } Almora Group 	Cambro-Ordovician granitoids Green phyllite, mica schist, carbonaceous schist, quartzite	~1000
Lesser Himalaya	Nathuakhan Formation [ca. 760 Ma] Berinag-Munsiari Formation [ca. 1800 Ma] Debguru Porphyry [ca. 1850 Ma] 	Green phyllite, lithic-rich quartzite Quartzite, schist, and mafic sill Granitoid gneiss	500
	Krol Formation [Ediacaran] Blaini Formation [Cryogenian] Nagthat Formation Chandpur Formation [<800 Ma] Bhowali Quartzite & Bhimal Volcanics [ca. 1860 Ma] Amritpur Granite Gneiss [1900 ± 100 Ma] 	Black and red shale, sandstone, and cherty limestone Gray and black shale, sandstone, and dolomite Muddy sandstone Muddy sandstone and mudstone Clean quartzite, and mafic sill Granite-granodiorite augen gneiss	2800 ~2050
Subhimalaya	upper member [4.5-1 Ma] middle member [11 - 4.5 Ma] lower member [13 - 11.5 Ma]	Coarsening up sequence of mudstone, sandstone, and conglomerate	~6000
	Lugad Gad (Dumri/Kasauli equivalent) [<22 - 13 Ma] 	Green sandstone, minor mudstone	300
Note: STDS—South Tibetan detachment system; MCT—Main Central thrust; MBT—Main Boundary thrust; MFT—Main Frontal thrust.			

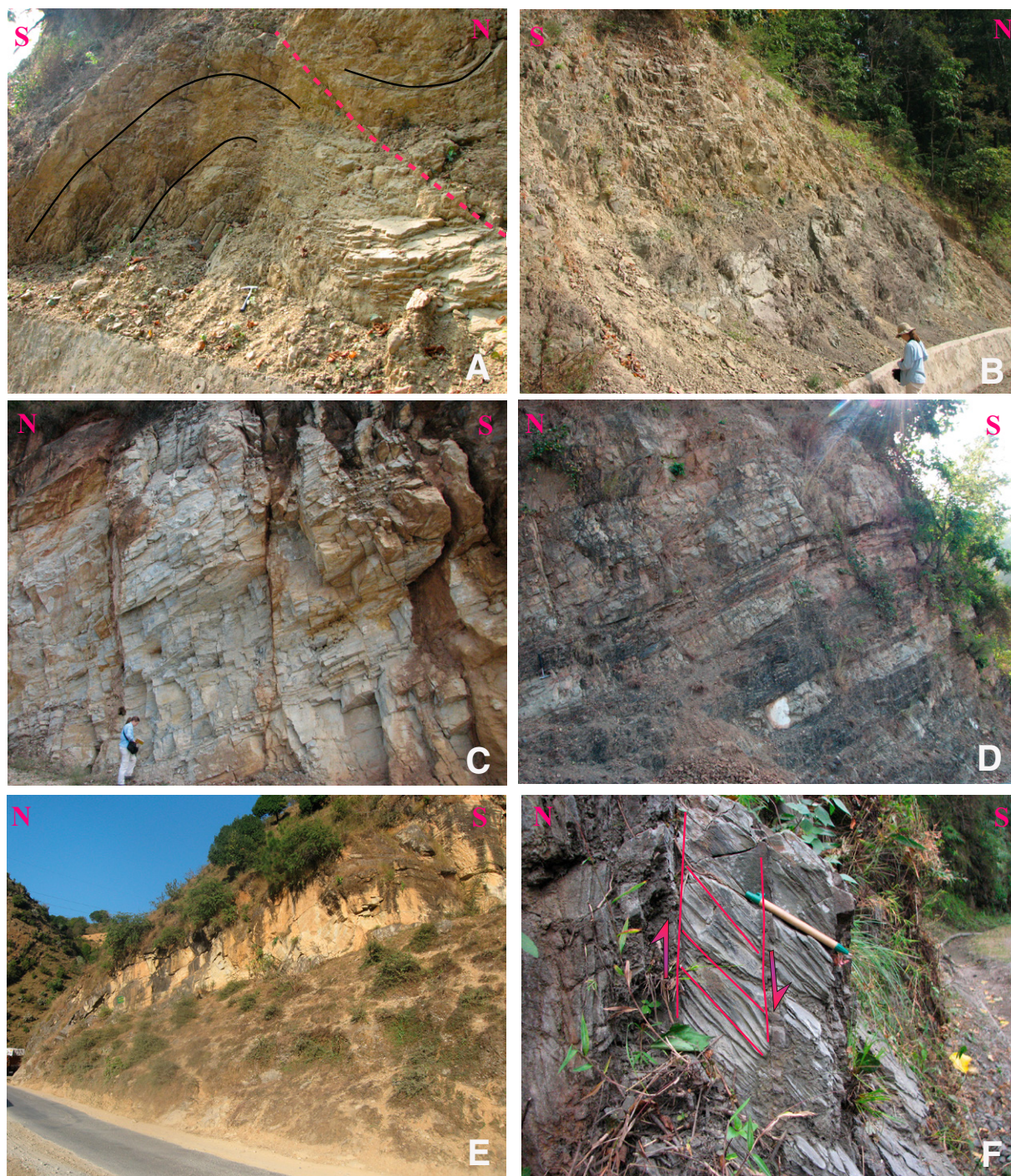


Figure 3. Subhimalayan and Lesser Himalayan rocks: (A) Thin-bedded mudstone of lower Siwalik unit, north of the Main Frontal thrust, with a south-vergent asymmetric fold. Red-dashed line demarcates a small-scale fault; 28-cm-long hammer for scale. (B) Bedded argillaceous sandstone, with paleosols (dark area) of Lugad Gad Formation; second author for scale. (C) North-dipping, bedded Berinag Quartzite from the southern limb of the Askot klippe; second author for scale. (D) An overall coarsening-upward sequence of alternating bedded micaceous quartzite and phyllite (turbidite), immediately north of the Almora klippe (sample SM11-022; see Fig. 2A); 28-cm-long hammer for scale. (E) North-dipping, thick-bedded dolomite of Deoban Formation, south of Pithoragarh (Fig. 2A); 2-m-wide road for scale. (F) Brittle fractured Mandhali Formation, phyllite with C-S surfaces, from north of the Askot klippe. Bedding planes (C) are planes of shear; 15 cm pen for scale.

a thickness of ~11 km as determined by previous studies (Srivastava and Mitra, 1994; C el erier et al., 2009) and from our mapping. An intra-Lesser Himalayan thrust, known as the Tons thrust, is interpreted to separate Paleoproterozoic–Mesoproterozoic lower Lesser Himalayan rocks to the north from the Neoproterozoic–Cambrian Lesser Himalayan rocks to the south (Srivastava and Mitra, 1994; Richards et al., 2005; C el erier et al., 2009).

Greater Himalaya

Greater Himalayan rocks consist of Neoproterozoic–Ordovician metasedimentary and meta-igneous rocks (Parrish and Hodges, 1996; DeCelles et al., 2000; Yin, 2006; Gehrels et al., 2011), which are intruded by Miocene leucogranite (Vison  and Lombardo, 2002; Searle et al., 2010; Godin and Harris, 2014). Greater Himalayan rocks north of the Main Central thrust are upper-amphibolite- to granulite-facies metasedimentary and meta-igneous rocks (Figs. 4B and 4C), known as the Vaikrita Group, and they are divided from structurally low to high into the Joshimath, Pandukeswar, and Badrinath Formations (Spencer et al., 2012a, 2012b; Iaccarino et al., 2017). The upper Badrinath Formation in the study area is known as Pindari Formation (Table 1). These three formations likely

correspond to Greater Himalaya Formations I, II, and III in central Nepal (Le Fort, 1974; Colchen et al., 1986), where a single formation may consist of different thrust sheets (e.g., Corrie and Kohn, 2011), and the three formations may be separated by tectono-metamorphic discontinuities (Carosi et al., 2016). Temperatures and pressures are as high as ~800  C and ~14 kbar in Greater Himalayan rocks north of the Main Central thrust in an ~500 km sector spanning central Nepal through Garhwal, west of our study area (Kohn, 2014).

Medium- to high-grade metamorphic rocks of Greater Himalayan affinity (i.e., Neoproterozoic depositional ages and less negative Nd isotopic values) also crop out within the Almora klippe (Mandal et al., 2015) carried by the Almora thrust. Valdiya (1980) described these rocks as an allochthonous unit that originated from the upper-amphibolite- to granulite-facies Greater Himalayan metamorphic rocks to the north (Fig. 4D). The Almora klippe is composed of metasedimentary rocks and Cambrian–Ordovician (ca. 500 Ma) granitoids. These rocks show greenschist to upper-amphibolite facies structurally upward with temperatures from 500  C to 700  C and pressures of 4–8 kbar (Joshi and Tiwari, 2009; Rawat and Sharma, 2011); thus, these pressure-temperature conditions are lower than Greater Himalayan rocks north of the Main Central thrust.

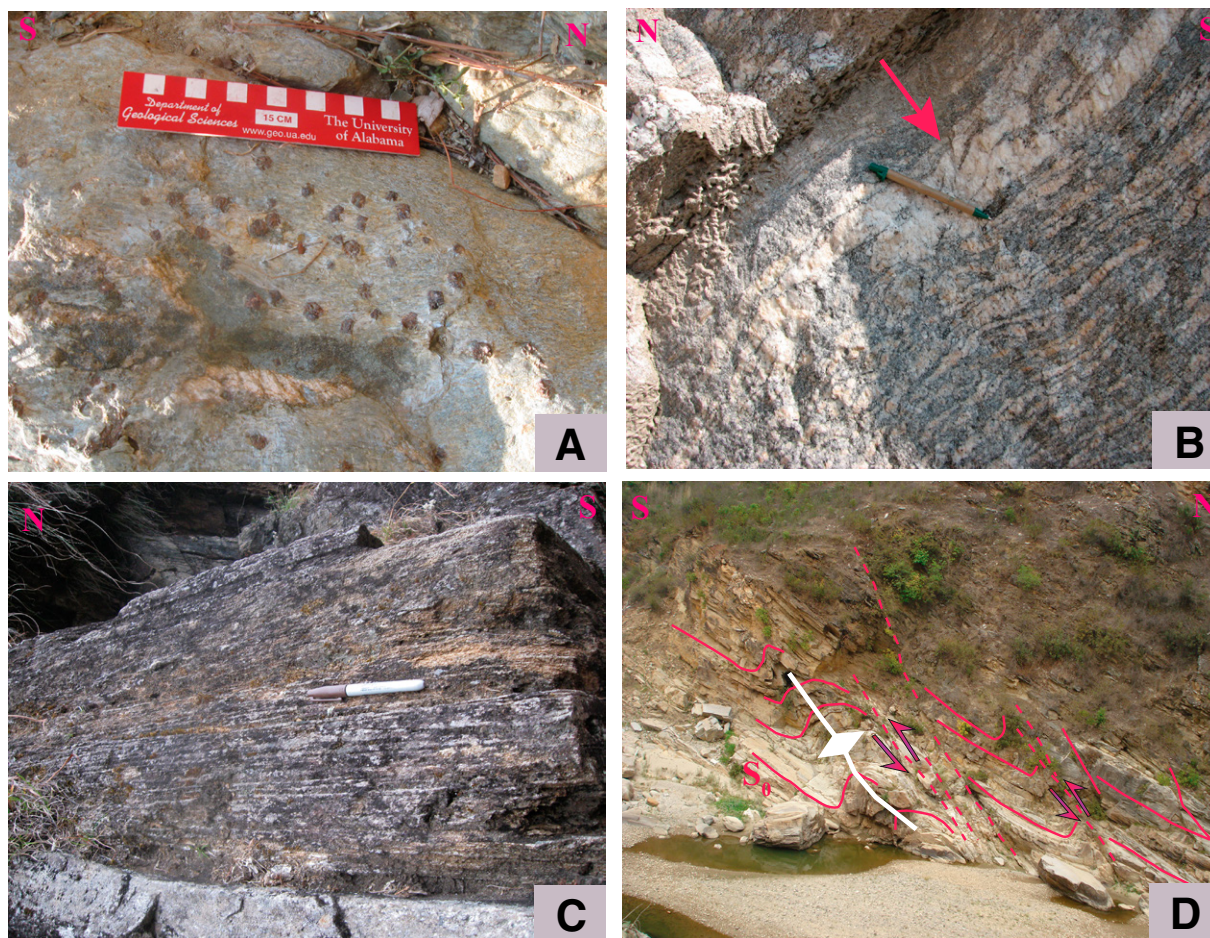


Figure 4. Metamorphic rocks in the field area: (A) Garnetiferous chlorite-muscovite schist from the Askot klippe with garnet porphyroblasts; 15 cm ruler for scale. (B) Mylonitic granite gneiss from Main Central thrust hanging wall, near Sobla (Fig. 2). Small-scale asymmetric fold within thicker (marked with a red arrow) layer shows top-to-the-south shear sense; 15 cm pen for scale. (C) Foliated calcisilicate Greater Himalayan gneiss, north of Sobla (Fig. 3); 10 cm marker for scale. (D) Asymmetrical fold on interbedded quartzite and phyllite, exposed in Kosi River bed from the southern margin of the Almora klippe. South-vergent folds indicate top-to-the-south shear sense.

TABLE 2. LOCALITY INFORMATION FOR THE SAMPLES USED IN U-Pb ZIRCON GEOCHRONOLOGY AND WHOLE-ROCK Nd ANALYSES

Sample	Coordinates		Unit	Lithology
	°N (dd.ddddd)	°E (dd.ddddd)		
SM11-032 (DZ)	29.798761	80.415655	Mandhali Formation	Pebbly quartzite
SM111-48 (IZ)	30.130862	80.245917	Munsiari Formation	Granite-granodiorite augen gneiss
SM11-58 (DZ)	29.458224	79.583645	Nathuakhan Formation	Gray quartzite with mud partings
SM11-59 (IZ)	29.436516	79.562599	Debguru Formation	Granite-granodiorite augen gneiss
SM11-035 (Nd)	30.068653	80.606967	Vaikrita Group (GH)	Pelitic schist
SM11-039 (Nd)	30.062817	80.587733	Munsiari Formation	Pelitic schist
SM11-046 (Nd)	30.166358	80.250152	Vaikrita Group (GH)	Pelitic schist/schistose gneiss
SM11-049 (Nd)	30.107226	80.243676	Munsiari Formation	Schistose gneiss

Note: DZ—detrital zircon; IZ—igneous zircon; Nd—neodymium; GH—Greater Himalaya.

METHODS

Zircon Geochronology

Four 1–2 kg samples were collected (for sample details, see Table 2) and processed for U-Pb isotopic analyses of igneous and detrital zircons. Zircons were separated using a jaw crusher, disk mill, water table, magnetic separator, and heavy liquids. A split of the zircon grains was mounted in epoxy together with Sri Lanka and R33 zircon standards (Gehrels et al., 2008). These mounts were polished to halfway through individual zircon grains and imaged using backscattered-electron and cathodoluminescence imaging at the University of Arizona. Zircons were analyzed for U-Pb ages (Table 2) using the laser ablation–inductively coupled plasma–mass spectrometer (LA-ICP-MS) at the University of Arizona LaserChron Center following methods described in Gehrels et al. (2006, 2008, 2011; see also GSA Data Repository Table DR1¹). Instrumentation included a 193 nm ArF excimer laser (Photon Machines Analyte G2) and a Nu HR multicollector (MC) ICP-MS. Spot sizes were 30 μm for U-Pb data and positioned relative to cathodoluminescence images to ensure that the ablation pits did not cross multiple age domains or inclusions. Data were standardized to Sri Lanka zircon (563 ± 3.2 Ma; 2σ), with a standardization error of $\sim \pm 1\%$. Ages were based on $^{207}\text{Pb}/^{206}\text{Pb}$, omitting highly discordant ($>30\%$ for detrital zircons) and compositionally anomalous data. Age uncertainties are reported both for precision and including a 1% standardization error. Uncertainties in the U-Pb decay systems are negligible.

Nd Isotopic Analysis

Four whole-rock metasedimentary rocks were collected and processed for whole-rock Nd isotopic analysis (Table 2). Samples were powdered in a ring and puck mill. Approximately 300 mg of powdered rock were digested for 1 wk in an $\sim 10:1$ HF:HNO₃ mixture in steel-jacketed polytetrafluoroethylene (PTFE) bombs in a standard convection oven at 160 °C. The samples produced a clear solution following bomb dissolution and conversion to chlorides. Samples were spiked with mixed ^{149}Sm - ^{150}Nd tracer, and Sm and Nd were isolated using established ion-chromatographic techniques (Patchett and Ruiz, 1987; Vervoort and Patchett, 1996). The isotopic analyses were performed at Washington State University using a Thermo Finnigan Neptune MC-ICP-MS. Elemental concentrations of Sm-Nd as well as parent/daughter ratios ($^{147}\text{Sm}/^{144}\text{Nd}$) were determined by isotope dilution using the same solution as the isotope composition

measurement, following the approach of Boelrijk (1968). Total uncertainty is estimated to be better than 0.003% for $^{143}\text{Nd}/^{144}\text{Nd}$ and 0.5% for $^{147}\text{Sm}/^{144}\text{Nd}$ (Vervoort et al., 2004). The four samples showed no evidence for partial melting, so we assume that the Nd isotopic characteristics are representative of the sedimentary protolith.

Mapping

We integrated our field data with the published map of Valdiya (1980), which was georeferenced using ArcMap 10.0TM, an ESRI mapping software package (Figs. 2A and 2B). A hillshade map was created using Advanced Spaceborne Thermal Emission and Reflection Radiometer (ASTER) Global Digital Elevation Model Version 2 (GDEM V2) data set (Data source: <http://asterweb.jpl.nasa.gov/gdem.asp>). The georeferenced map was draped over the hillshade map to cross-check the georeferencing. We mapped structures and lithologies at scales of 1:50,000 and 1:100,000 along an ~ 150 -km-long, north-to-south traverse between the South Tibetan Detachment system and the Main Frontal thrust. We incorporated the maps of the Chiplakot klippe (Patel et al., 2007, 2011), the Askot klippe (Mandal et al., 2016), and the South Tibetan Detachment system (Patel et al., 2011) in our geological map (Fig. 2A).

Balanced Cross-Section Construction, Assumptions, and Limits

Balanced cross section is a powerful tool for interpreting complex structures, especially in the external parts of fold-thrust belts with sparse data. Restoration validates a balanced cross section and estimates the minimum shortening or extension. Line-length-balanced cross sections assume that line lengths are conserved during deformation (Dahlstrom, 1969; Suppe, 1983; Dahlen, 1990). Line-length balancing has been successfully applied in the Himalayan fold-thrust belt (Coward and Butler, 1985; Schelling and Arita, 1991; Srivastava and Mitra, 1994; DeCelles et al., 1998, 2001, 2016; Robinson et al., 2006; Long et al., 2011; Khanal and Robinson, 2013; Webb, 2013; Robinson and Martin, 2014; Bhattacharyya et al., 2015a; Parui and Bhattacharyya, 2018) to determine the structural and kinematic evolution, to interpret inverted metamorphism, and to infer later exhumation processes of the metamorphic core.

We constructed a balanced cross section using a flat-ramp-flat geometry for the Main Himalayan thrust, based on a recent common conversion point receiver function image (Caldwell et al., 2013), 125 km west of our cross section. This image reveals that the shallower Main Himalayan thrust flat lies ~ 10 km below sea level and dips north at $\sim 2^\circ$, connecting to an ~ 10 -km-high midcrustal ramp that dips north at $\sim 16^\circ$. The deeper Main Himalayan thrust flat lies ~ 20 km below sea level and dips north at $\sim 4^\circ$ (Caldwell et al., 2013). The cross section was pinned in the south by projecting the depth of the basal, undeformed Siwalik Group in the

¹GSA Data Repository Item 2019153, Table DR1: U-Pb zircon data, is available at <http://www.geosociety.org/datarepository/2019>, or on request from editing@geosociety.org.

foreland Ujhani well (Sastri et al., 1971), 151 km SSW of Tanakpur, India (Fig. 2A), at an angle $\sim 2.0^\circ$. Based on calculated thicknesses of the Subhimalayan rocks that crop out within various Subhimalayan thrust sheets in the study area, or in adjacent areas (Raiverman, 2002), we determined the footwall template and estimated the Main Himalayan thrust depth at ~ 6 km below the Main Frontal thrust. In addition, from the Main Boundary thrust hanging-wall lithologies, we deduced that the entire Lesser Himalayan sequence is in the Main Boundary thrust footwall and continues southward below Subhimalayan rocks. The cross section is oriented N15E, nearly parallel to the transport direction, as determined from trends of small-scale fold axes that we assumed to be orthogonal to the transport direction (e.g., Parui and Bhattacharyya, 2018). We estimated the true thickness of the individual thrust sheets from the mean foliation dip of the thrust sheet, exposed (outcrop) width of the thrust sheet, and slope of the transect. Apparent foliation and bedding dips were calculated from surface measurements and projected along strike onto the cross section. Axial planes of highest-order, fault-bend folds from each thrust sheet were determined by bisecting the interlimb angle at the hinges, and most axial planes were drawn using the kink method (Suppe, 1983).

Additional assumptions in constructing cross sections included the following: (1) Micro- and mesoscale deformation (e.g., Figs. 3 and 4), which is dominated by shortening structures, was not taken into consideration for any units because of the difficulty in quantifying shortening amounts; (2) Greater Himalayan rock was restored as a slab, although

Greater Himalayan rocks exhibit evidence for prior ductile/plastic deformation, such as grain boundary sliding, shearing, and folding (e.g., Jain et al., 2002); and (3) shortening from intra-Greater Himalayan thrusts (e.g., see Montomoli et al., 2013, 2015; Larson et al., 2015; Carosi et al., 2018) was not incorporated in the shortening estimates. These three assumptions ensure that shortening estimates are minima. Folding of the overlying roof thrusts resulted from formation of the Lesser Himalayan duplex. These large-scale folds are only shown in our cross section. When constructing the cross section, unknowns included: (1) positions of hanging-wall cutoffs of the thrust sheets, because they have all been eroded, (2) the length of the longer thrust sheets, because of erosion of their more distal tips, and (3) the position of the northern cutoff of the Lesser Himalayan rocks, which is unknown, and, thus, shortening could have been much greater. Minimum bed lengths were used in the cross section to minimize shortening, assuming that the hanging-wall cutoffs are immediately above the present-day erosional surface.

RESULTS

Zircon Geochronology and Nd Isotopic Analyses

Sample SM11-032 is from a pebbly quartzite bed (Figs. 2A and 5A) within the carbonaceous slate/phyllite of the Mandhali Formation. The age spectra show clusters around ca. 1800 Ma and ca. 2500 Ma (Fig. 5B) with

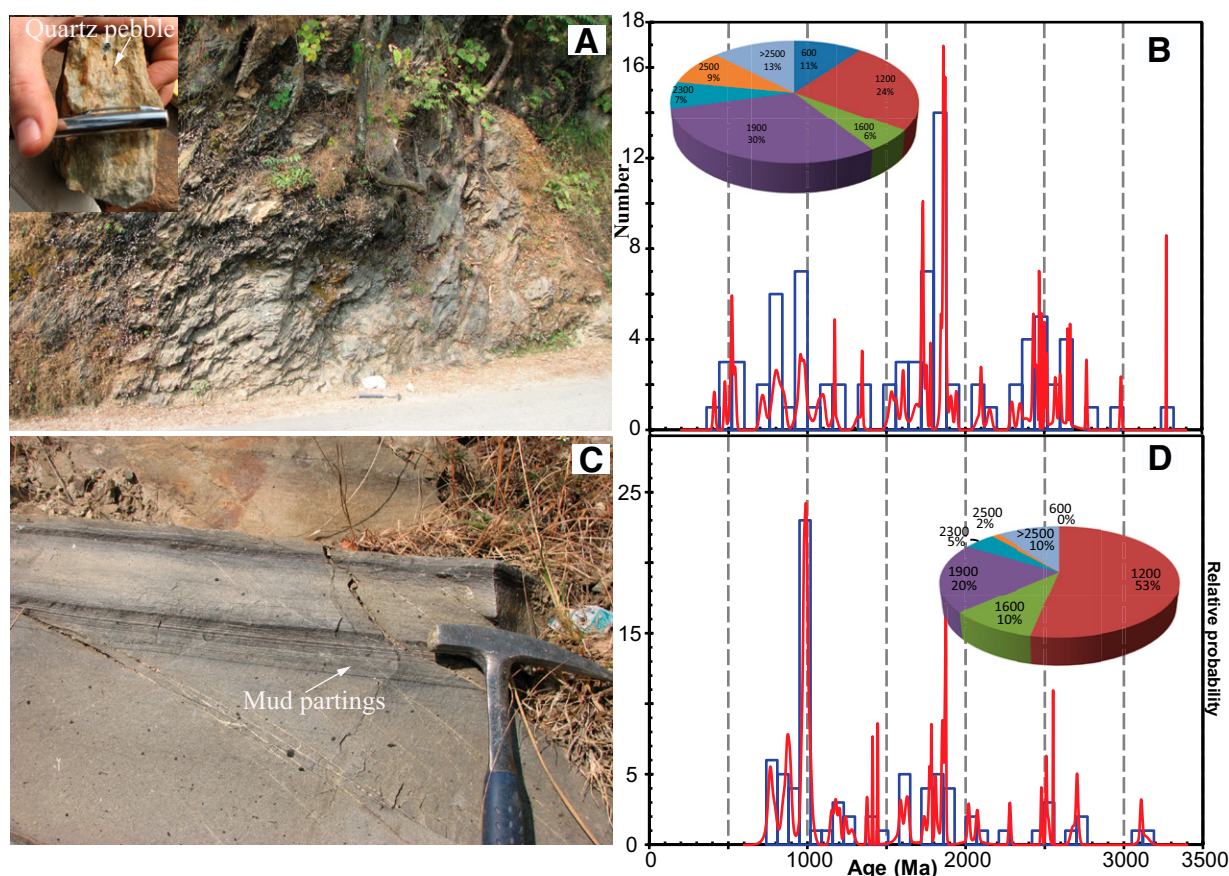


Figure 5. (A) Photographs of SM11-032, a pebbly quartzite. Inset shows rock texture; 5-cm-long pen top for scale. Field photo of outcrop includes a 28-cm-long hammer lying on the road for scale. (B) SM11-032 detrital zircon age spectrum with pie chart (inset), showing distribution of age populations. (C) Photograph of SM11-058, a micaceous quartzite; 28-cm-long hammer for scale. (D) SM11-058 detrital zircon age spectrum and pie chart of age populations (inset).

a tail toward younger ages, terminating at ca. 500 Ma. To determine the depositional age, we used the approach of Martin et al. (2011), adding the uncertainty (including standardization errors) and rounding up to the nearest 10 Ma. Thus, we interpret the maximum depositional age of ca. 500 Ma.

Sample SM11-058 is a micaceous sandstone (or quartzite) containing internal mud drapes (Fig. 5C) from the Nathuakhan Formation, likely a facies variant of the ca. 800 Ma Chandpur Formation mapped by C el erier et al. (2009) south of the Almora klippe (Fig. 2B). The age spectra show age clusters around ca. 1000 Ma, 1800 Ma, and 2500 Ma (Fig. 5D). Four younger zircons yielded ages between 765 and 751 Ma with more than 90% concordance at 1σ . Following the approach of Martin et al. (2011), we infer a maximum depositional age of ca. 760 Ma.

Sample SM11-048 is granite–augen gneiss (Figs. 2B and 6A) from the hanging wall of what Valdiya (1980) mapped as the Munsiri thrust (Fig. 2). This sample yielded a mean crystallization age of 1860 ± 19 Ma (with ± 1 standardization $^{206}\text{Pb}/^{207}\text{Pb}$ error, $n = 17$, both cores and rims; Fig. 6B), with no inherited core older than ca. 1850 Ma.

Sample SM11-059 is from the Debguru porphyry (Fig. 6C) of the Ramgarh Group, 50 km west of our cross-section line (Fig. 2B). This sample yielded a mean crystallization age of 1867 ± 20 Ma (with ± 1 standardization $^{206}\text{Pb}/^{207}\text{Pb}$ error, $n = 15$, core and rims), with no inherited cores older than ca. 1850 present (Fig. 6D).

Samples from the Munsiri Formation, SM11-039 and SM11-049, yielded very negative ϵ_{Nd} values of -22.9 and -25.6 , respectively. Samples from the lower part of the Greater Himalaya (Joshimath Formation), SM11-035 and SM11-046, yielded less negative ϵ_{Nd} values of -16.1 and -15.1 , respectively (Fig. 2A; Table 3).

Structural Mapping

Field mapping (Srivastava and Mitra, 1994; C el erier et al., 2009; this study) reveals, from north to south, the following major structures: Main Central thrust, Ramgarh-Munsiri thrust, Lesser Himalayan duplex, Main Boundary thrust, and Main Frontal thrust, similar to other parts of the

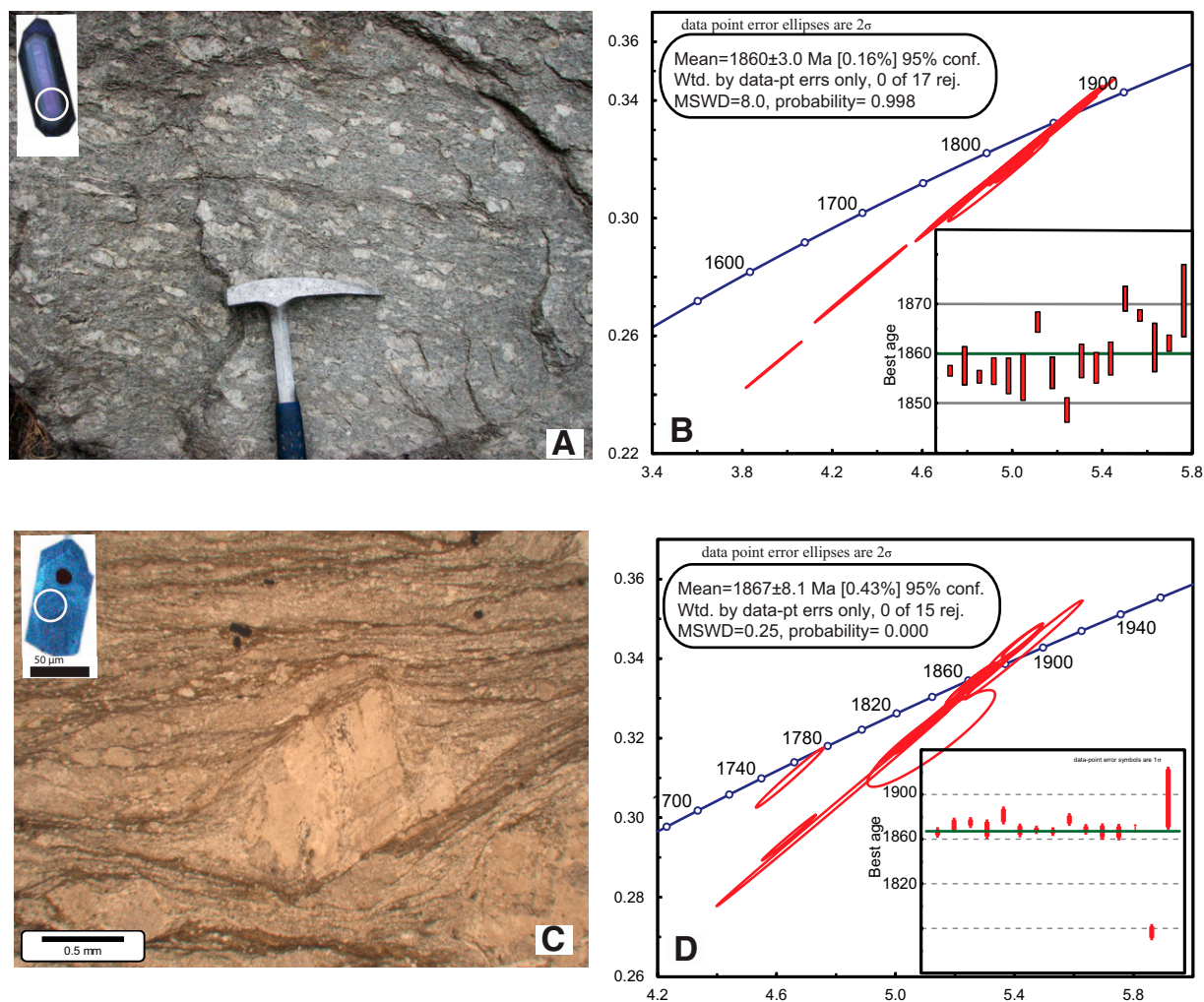


Figure 6. (A) Outcrop photograph of sample SM11-048, a granitoid augen gneiss from the Ramgarh-Munsiri thrust sheet, north of Munsiri; 28 cm hammer for scale. Inset shows a cathodoluminescence (CL) image of a separated zircon prior to analysis and an analytical location (circle). (B) U-Pb concordia plot and weighted average (inset) of SM11-048. (C) Thin-section photomicrograph of sample SM-059 (Debguru porphyry of Ramgarh-Munsiri thrust sheet, southern footwall of the Almora klippe) showing intense mylonitization. Inset shows CL image of a separated zircon prior to analysis and an analytical location (circle). (D) U-Pb concordia plot and weighted average (inset) of SM11-059. MSWD—mean square of weighted deviates.

TABLE 3. WHOLE-ROCK Nd ISOTOPIC ANALYSIS RESULTS

Sample	Sm (ppm)	Nd (ppm)	$^{147}\text{Sm}/^{144}\text{Nd}$	$^{143}\text{Nd}/^{144}\text{Nd}$	\pm (abs std err)	$\epsilon_{\text{Nd}(0)}$	\pm
SM11-035	5.96	31.9	0.1129	0.511805	0.000005	-16.0	0.10
SM11-039	6.48	32.8	0.1193	0.511454	0.000007	-22.9	0.14
SM11-046	5.09	25.4	0.1213	0.511854	0.000006	-15.1	0.12
SM11-049	8.29	50.5	0.0992	0.511320	0.000006	-25.5	0.12

Himalaya. The South Tibetan Detachment system is too far north (~20 km NW of Sobla; Fig. 2A) and in restricted areas to be reached easily; thus, we incorporated the structural fabrics and location of the South Tibetan Detachment system from Patel et al. (2011).

Main Central Thrust Sheet

The Main Central thrust sheet carries Greater Himalayan rocks and is bounded by the South Tibetan Detachment system in the north and Main Central thrust in the south. Originally defined by Heim and Gansser (1939), the Main Central thrust in this region is known as the Vaikrita thrust, a discrete structure that places high-grade Greater Himalayan rocks atop lower-grade Lesser Himalayan rocks. However, the lack of a general consensus in defining this high-strain zone had led to different ways of defining the Main Central thrust (see Searle et al., 2008; Martin, 2016). In this study, we follow the definition of the Main Central thrust as a high-strain zone with a compressed metamorphic gradient (e.g., Le Fort, 1975; Martin, 2016) with distinct whole-rock Nd isotopic values and U-Pb ages in the hanging wall versus the footwall. In our field area, the Main Central thrust (Fig. 2A) places thick bands of garnetiferous schist with segregated quartz veins and banded gneiss on top of quartzose schists of the Paleoproterozoic Lesser Himalayan Munsiri Formation. We mapped the Main Central thrust, north of Sobla and Munsiri, as a tectono-stratigraphic boundary, juxtaposing rocks with less negative ϵ_{Nd} values (-16.0 to -15.1) against rocks with very negative ϵ_{Nd} values (-22.9 and -25.5; Fig. 2A).

Greater Himalayan rocks exhibit penetrative ductile fabrics (Figs. 4B and 4C), indicating penetrative ductile deformation. In the hanging wall of the Main Central thrust, schistosity and gneissosity are the primary foliation types, and they are generally parallel to the axial planes of the small-scale mesoscopic folds. The foliations dip 55–75°N. Small-scale crenulations have axes that plunge 35–65°NE. Schistosity and gneissosity within the Greater Himalayan rocks north of the Main Central thrust are generally parallel to bedding and tectonic foliations of Paleoproterozoic Lesser Himalayan rocks in the footwall of the Main Central thrust. The thickness of Greater Himalayan rock ranges between 11 and 17 km. To the west in Garhwal, peak metamorphic temperatures range between 800 °C and 850 °C throughout Greater Himalayan rocks, whereas pressure increases from 12 to 14 kbar at 3 km above the Main Central thrust and then decreases to 9 kbar near the South Tibetan Detachment system (Spencer et al., 2012a).

Ramgarh-Munsiri Thrust Sheet

The Ramgarh-Munsiri thrust is a crustal-scale intra-Lesser Himalayan thrust that carries Paleoproterozoic Ramgarh and Munsiri Formations and forms the floor thrust of a coupled roof thrust system of the Lesser Himalayan duplex (Robinson and Pearson, 2013). In Garhwal-Kumaun, this thrust has been mapped as two separate thrusts, the Munsiri thrust to the north and Ramgarh thrust to the south (Valdiya, 1980; Srivastava and Mitra, 1994; Ahmad et al., 2000). The Berinag thrust (e.g., Valdiya, 1980) also carries Paleoproterozoic rocks (McKenzie et al., 2011; Mandal et al., 2015, 2016) and may be structurally equivalent to the Ramgarh-Munsiri thrust. Hanging-wall Paleoproterozoic rocks in all of these thrusts

include quartzite (Fig. 3C), schist/phyllite, and augen gneiss. The contacts between the Paleoproterozoic granitoids and metasedimentary rocks along the Himalaya vary from intrusive to sheared (Bhattacharyya et al., 2015b; Das et al., 2016; Mandal et al., 2016). In our study area, one of these contacts at the southern margin of the Askot klippe is sheared and juxtaposes 1857 ± 19 Ma granite-granodiorite gneiss atop a sequence of metasedimentary and metavolcanic rocks (Mandal et al., 2016). These granitoids and associated metasedimentary rocks are part of a Paleoproterozoic continental arc (Kohn et al., 2010; Mandal et al., 2016), and their degree of deformation varies from practically undeformed to mylonitic, with substantial grain-size reduction near major thrusts.

To the north, in the immediate footwall of the Main Central thrust, we mapped two thrust sheets (Fig. 2A) based on the repetition of Munsiri Formation—equivalent Paleoproterozoic Lesser Himalayan rocks. The structurally higher thrust sheet is ~5 km thick and contains amphibolite-facies paragneiss, schistose quartzite, schist, and minor quartzite. North of the Chiplakot klippe, the structurally lower thrust sheet is ~5 km thick and contains ~500 m bands of dolomite and calcisilicate, along with quartzite and schist. These carbonate rocks are also part of the Munsiri Formation, similar to what is reported in far western Nepal (Robinson et al., 2006). Bedding and schistosity are parallel to Greater Himalayan rocks with an average of 280/60°N near Sobla, while south of Munsiri, the average foliation is 230/50°NW, suggesting regional folding of the foliation. Axes of small-scale folds, and crenulation lineations trend/plunge toward the NNW, while stretching lineations trend/plunge toward the NNE. The lower thrust sheet also exhibits changes in foliation strike between Sobla and Munsiri (Fig. 2A), nearly parallel to the upper thrust sheet. Schistosity-parallel centimeter-scale quartz veins that are folded and boudinaged are common within both these Paleoproterozoic Lesser Himalayan thrust sheets.

Between the Lesser Himalayan Paleoproterozoic rocks to the north and Almora klippe to the south (Fig. 2A), the Berinag thrust carries a sequence of ca. 1800 Ma quartzite, schistose quartzite, minor schist, and 1857 ± 19 Ma granite-granodiorite gneiss (Figs. 3C and 4A) and forms the Chiplakot and Askot klippen (Mandal et al., 2016). Metamorphic grade ranges from greenschist to amphibolite facies. In the Askot klippe, the southern limb dips 35°N, while the northern limb dips 60°–75°S, and the axis of this syncline plunges NW (Mandal et al., 2016). Another klippe of the Berinag thrust sheet crops out south of the Askot klippe, and it is dominantly composed of quartzite and schistose quartzite (Fig. 2A).

The Ramgarh-Munsiri thrust and its hanging-wall rocks crop out in the northern and southern footwall of the Almora thrust in the Almora klippe (Figs. 2A and 2B). Schist, schistose quartzite, and lenses of granite are common north of the klippe, while green phyllite and granitoids are common south of the klippe. The Deb guru porphyry is an L-S tectonite with abundant K-feldspar augen in the southern limb (Figs. 2A, 2B, and 6C). Bedding and foliation dips are 50–80°SW in the northern limb, whereas the dips in the southern limb are 28–58°N-NE.

Lesser Himalayan Duplex

The Lesser Himalayan duplex, consisting of Lesser Himalayan rocks, lies between the Paleoproterozoic Lesser Himalayan rocks of the Ramgarh-Munsiri thrust footwall to the north and the Almora klippe to the south, as well as underneath the Paleoproterozoic Lesser Himalayan rocks of the Chiplakot and Askot klippen. Major faults within and structurally above the Lesser Himalayan duplex were identified in the field based on sharp lithological breaks, abrupt changes in metamorphic grade, presence of shear fabrics, and/or repetition of stratigraphy. The duplex is composed of thrust sheets containing the Deoban + Mandhali Formations, Rautgara + Chakrata Formations, and the Ramgarh-Berinag-Munsiri Formations (as inferred from field mapping and balanced cross sections). North of

the Almora klippe, the Paleoproterozoic Rautgara Formation (Fig. 3D) is exposed with overall northward dips. Small-scale mesoscopic folds, with northerly dipping axial planes, were also observed. The northern contact of the Rautgara Formation was mapped as a normal fault as the stratigraphically younger Deoban Dolomite dips to the south (Fig. 2A). North of this structure until the southern limb of the Askot klippe is reached, thick- to thin-bedded rocks of the Deoban (Figs. 2 and 3E) and Mandhali Formations (Fig. 3F) are exposed. Bedding dips of the Mandhali Formation are 12–36°N at the southern end of the Askot klippe (Fig. 2A). North of the Askot klippe, Deoban and Mandhali Formation rocks (Fig. 3F) are locally known as the “calc zone of Tejam” (Heim and Gansser, 1939), and they exhibit variable foliation dips and dip directions.

Almora Klippe

South of the Lesser Himalayan duplex, the Almora klippe is composed of schist, gneiss, and quartzite with Greater Himalaya affinity ($\epsilon_{Nd} = -11.8$; Mandal et al., 2015) and a WNW-ESE-trending, doubly plunging axis. This klippe has been referred to as the lower Ramgarh nappe (i.e., thrust sheet) and overlying Almora nappe (Joshi and Tiwari, 2009). Schistosity and gneissosity in the Almora thrust sheet are parallel to the underlying Ramgarh-Munsiari thrust sheet. Ductile shearing has produced small-scale folding (Fig. 4D) with axial planes parallel to the regional foliation (S_1) and top-to-the-south vergence. Dips on the northern limb are 40–65°S-SW, while on the southern limb, dips are 32–62°N-NE.

Lesser Himalayan Imbricate Zone

The Lesser Himalayan imbricate zone is exposed in the area between south of the Almora klippe and north of the Main Boundary thrust. The zone contains intensely fractured quartzite and mafic sills, locally known as Bhowali quartzite and Bhimtal volcanics, respectively. These are likely Paleoproterozoic Rautgara-equivalent rocks (Mandal et al., 2015) and were carried in the Main Boundary thrust hanging wall (Fig. 2A) as an imbricate thrust sheet. A similar damage zone is reported 55 km to the northwest in the immediate hanging wall of the Main Boundary thrust (Shah et al., 2012). The northern thrust of the Lesser Himalayan imbricate zone juxtaposes the Neoproterozoic Nagthat Formation against Paleoproterozoic Rautgara equivalent rocks that crop out in the immediate Main Boundary thrust hanging wall (Fig. 2A). A broad syncline exposes the Neoproterozoic–Cambrian Lesser Himalayan Blaini and Krol Formations west of the cross-section line in the down-plunge direction (Fig. 2A).

Subhimalayan Thrust System

Between the Main Boundary thrust to the north and Main Frontal thrust to the south, the Subhimalayan thrust system consists of three thrust sheets, based on structural repetitions of similar lithofacies associations (Fig. 2A). The Main Frontal thrust is not exposed in Kumaun, but its location is inferred at the abrupt increase in slope from the Indo-Gangetic plain to the foothills. Beds dip at 19–52°N between the Main Frontal thrust and Main Dun thrust. A small splay of Main Dun thrust was mapped based on repetition of Lugad Gad Formation strata (Fig. 2A). Rocks north of this Main Dun thrust dip 55–78°N. Overall north-dipping beds within Subhimalayan thrust sheets suggest that only north-dipping limbs are preserved at the current erosional level.

INTERPRETATIONS

Lesser Himalayan Stratigraphic Ambiguity

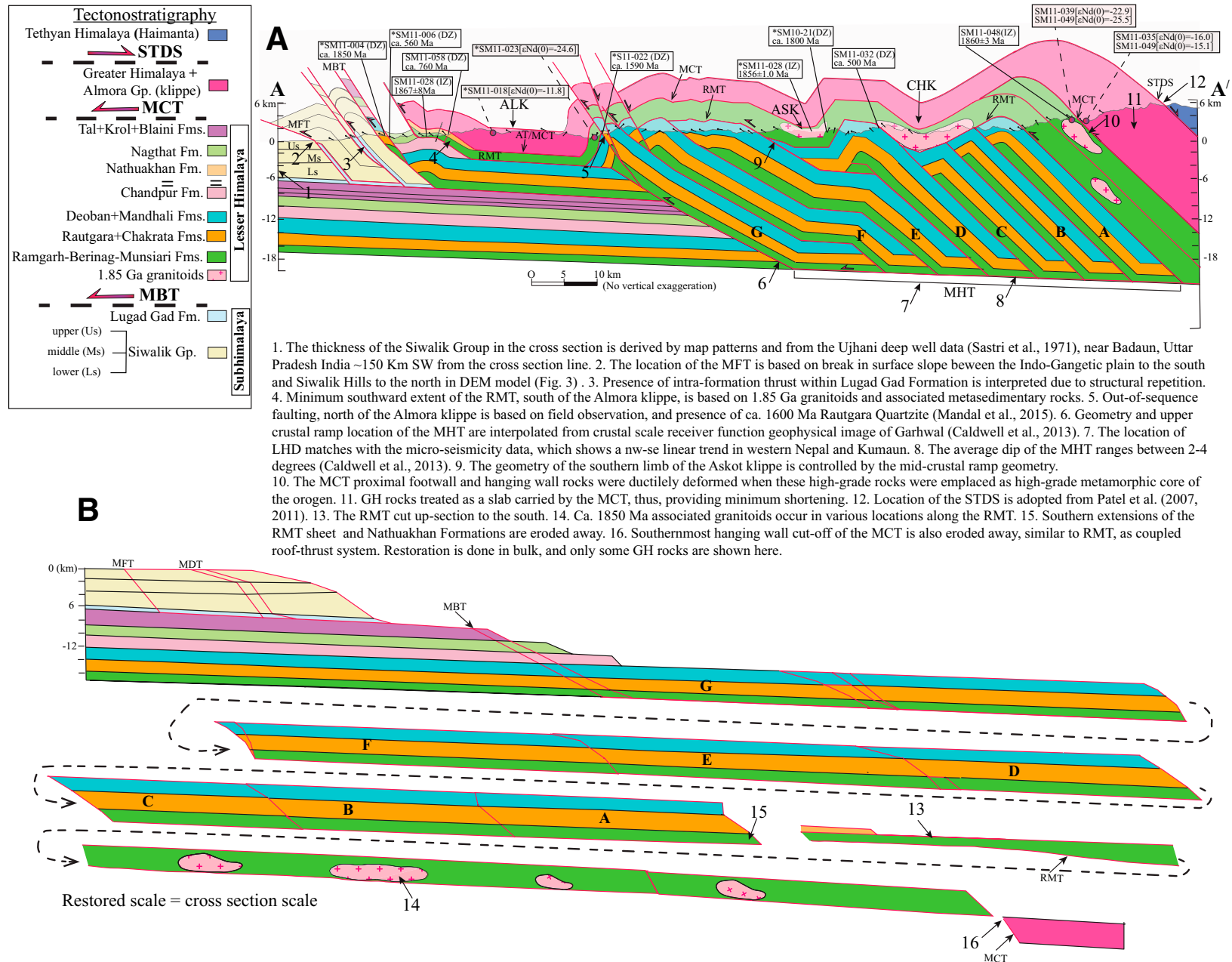
In the past, the terms “inner” and “outer” have been used to designate the geographic locations of Lesser Himalayan stratigraphy with respect

to the Tons thrust (see C  lerier et al., 2009, and references therein). The Tons thrust has been mapped as terminating at the NW end of the Almora klippe (Srivastava and Mitra, 1994; Fig. 1B). However, C  lerier et al. (2009) extended the Tons thrust to approximately our mapped position of the Ramgarh-Munsiari thrust immediately north of the Almora klippe (near sample SM11-022; Fig. 2A). Here, we recommend that “inner” versus “outer” be discontinued because stratigraphic level or age is useful for interpreting structure, and “inner” and “outer” obscure the structural significance of stratigraphic repetitions within the thrust belt. Based on U-Pb detrital zircon data, Mandal et al. (2015) showed that Paleoproterozoic strata crop out south of the Almora klippe, which implies that the Lesser Himalayan duplex and the Lesser Himalayan imbricate zone control the distribution of Lesser Himalayan rocks, not the Tons thrust. In addition, an intra-Lesser Himalayan Tons thrust (Richards et al., 2005) would have juxtaposed the Paleoproterozoic with Neoproterozoic Lesser Himalayan rocks before emplacement of the Almora klippe (= Main Central thrust; C  lerier et al., 2009) or movement along the Ramgarh-Munsiari thrust. This scenario would make the Main Central thrust and Ramgarh-Munsiari thrust out-of-sequence thrusts. No evidence exists for this kinematic interpretation either in our field area or elsewhere along strike in the Himalaya.

South of the Almora klippe in the Ramgarh-Munsiari thrust hanging wall, sample SM11-058 (Figs. 2B and 7A) is from a micaceous quartzite/sandstone, unconformably overlying the ca. 1850 Ma Deb guru porphyry (Mandal et al., 2015), and it yielded a ca. 760 Ma depositional age (Fig. 5D). This ca. 760 Ma depositional age is younger than the reported depositional ages along strike, i.e., ca. 800 Ma (C  lerier et al., 2009) and ca. 880 Ma (Mandal et al., 2015). We interpret this ca. 760 Ma unit as the Nathuakhan Formation, which is likely a distal facies variant of the Chandpur Formation (C  lerier et al., 2009). We assign it to the Ramgarh-Munsiari thrust sheet where Deb guru porphyry unconformably underlies the Nathuakhan Formation (Figs. 2A, 2B, 7A, and 7B). We further interpret that the Ramgarh-Munsiari thrust sheet is folded underneath the Almora klippe and crops out south of the Almora thrust, where it contains some younger, Neoproterozoic Nathuakhan Formation strata. In contrast, the Ramgarh-Munsiari thrust sheet in far western Nepal carries only the Paleoproterozoic Kushma and Ranimata Formations, and it is folded underneath the Dadeldhura klippe. Kumaun is the first location along the Himalayan arc where the Ramgarh-Munsiari thrust carries rocks younger than Paleoproterozoic.

Tectono-Stratigraphic Characterization of Klippen Rocks

The klippen of the Kumaun region provide insights into tectonic interpretations not possible elsewhere. The doubly plunging synclinal Almora klippe is the most structurally and stratigraphically complicated of all klippen within the Lesser Himalayan tectono-stratigraphic zone because it structurally rests on a coupled thrust system, consisting of the structurally higher Almora thrust (= Main Central thrust) and structurally lower Ramgarh-Munsiari thrust. Previous structural models (Srivastava and Mitra, 1994; C  lerier et al., 2009) followed the interpretation of Valdiya (1980) that the entire Almora klippe is the southward continuation of the Ramgarh-Munsiari thrust sheet. However, relatively young U-Pb ages (ca. 810–510 Ma; Fig. 2A) and less negative whole-rock ϵ_{Nd} values (~ -11 ; Figs. 2A and 2B) demonstrate that the Almora klippe represents the southern continuation of the Main Central thrust sheet or possibly an intra-Greater Himalayan thrust sheet carrying Greater Himalaya-affinity rocks (Mandal et al., 2015). Thus, the North and South Almora thrusts (Fig. 2A) are the Main Central thrust or an intra-Greater Himalayan thrust. Paleoproterozoic rocks are present underneath these Greater Himalayan rocks on the north and south sides of the klippe (Figs. 2A and 2B), and they are



1. The thickness of the Siwalik Group in the cross section is derived by map patterns and from the Ujhani deep well data (Sastri et al., 1971), near Badaun, Uttar Pradesh India ~150 Km SW from the cross section line. 2. The location of the MFT is based on break in surface slope between the Indo-Gangetic plain to the south and Siwalik Hills to the north in DEM model (Fig. 3). 3. Presence of intra-formation thrust within Lugad Gad Formation is interpreted due to structural repetition. 4. Minimum southward extent of the RMT, south of the Almora klippe, is based on 1.85 Ga granitoids and associated metasedimentary rocks. 5. Out-of-sequence faulting, north of the Almora klippe is based on field observation, and presence of ca. 1600 Ma Rautgara Quartzite (Mandal et al., 2015). 6. Geometry and upper crustal ramp location of the MHT are interpolated from crustal scale receiver function geophysical image of Garhwal (Caldwell et al., 2013). 7. The location of LHD matches with the micro-seismicity data, which shows a nw-se linear trend in western Nepal and Kumaun. 8. The average dip of the MHT ranges between 2-4 degrees (Caldwell et al., 2013). 9. The geometry of the southern limb of the Askot klippe is controlled by the mid-crustal ramp geometry. 10. The MCT proximal footwall and hanging wall rocks were ductilely deformed when these high-grade rocks were replaced as high-grade metamorphic core of the orogen. 11. GH rocks treated as a slab carried by the MCT, thus, providing minimum shortening. 12. Location of the STDS is adopted from Patel et al. (2007, 2011). 13. The RMT cut up-section to the south. 14. Ca. 1850 Ma associated granitoids occur in various locations along the RMT. 15. Southern extensions of the RMT sheet and Nathuakhan Formations are eroded away. 16. Southernmost hanging wall cut-off of the MCT is also eroded away, similar to RMT, as coupled roof-thrust system. Restoration is done in bulk, and only some GH rocks are shown here.

Figure 7. (A–B) Regional balanced cross section (A) and restored section (B) along line A–A' in Figure 2. A–G indicate thrust sheets within the Lesser Himalayan duplex. For sample identifications, IZ—igneous zircon sample; DZ—detrital zircon sample. Abbreviations: ALK—Almora klippe; AT—Almora thrust; ASK—Askot klippe; CHK—Chiplakot klippe; DEM—digital elevation model; GH—Greater Himalaya; LHD—Lesser Himalayan duplex; MBT—Main Boundary thrust; MCT—Main Central thrust; MDT—Main Dun thrust; MFT—Main Frontal thrust; MHT—Main Himalayan thrust; RMT—Ramgarh-Munsiari thrust; STDS—South Tibetan Detachment system. Asterisk (*) on sample numbers denotes zircon and whole-rock neodymium stratigraphic projected sample locations of Mandal et al. (2015, 2016).

carried by the Ramgarh-Munsiari thrust, which is folded along with the Main Central thrust sheet to form the klippe (Fig. 7A). In the footwall of the South Almora thrust (Main Central thrust), the basal part of the Ramgarh-Munsiari thrust sheet is composed of rocks with crystallization ages of 1867 ± 20 Ma (sample SM11-059, Debguru porphyry) and 1869 ± 19 Ma (sample SM11-009), and they are unconformably overlain by Neoproterozoic Nagthat and Chandpur-equivalent (Nathuakhan Formation) rocks (SM11-006, SM11-058; Figs. 2B and 7A). In the footwall of the North Almora thrust (Main Central thrust), metasedimentary rocks with very negative ϵ_{Nd} values (-24.6 ; Fig. 2A) crop out. While previous studies distinguished the Ramgarh thrust (= Ramgarh-Munsiari thrust) on the south side of the Almora klippe, they did not identify the Ramgarh-Munsiari thrust on the north side of the klippe because the Ramgarh-Munsiari thrust sheet rocks appear similar in outcrop to the overlying Greater Himalaya-affinity rocks (Valdiya, 1980; Srivastava and Mitra, 1994; C  lerier et al., 2009). Geochronology and isotope geochemistry allowed the Ramgarh-Munsiari thrust Lesser Himalayan rock to be identified on both sides of the klippe (Mandal et al., 2015; this study).

Between the Almora and Askot klippen, the Berinag thrust emplaces predominantly ca. 1800 Ma quartzite with minor schist atop the younger Deoban and Mandhali Formations (Fig. 2A). Because the Berinag thrust carries Paleoproterozoic rock (sample NDIC, ca. 1800; McKenzie et al., 2011), it occupies a similar structural position as the Ramgarh-Munsiari thrust. Similarly, the Berinag thrust carries the Askot klippe and emplaces 1857 ± 19 Ma igneous rocks (granite-granodiorite gneiss; SM11-028 IZ; Fig. 2A) and ca. 1800 Ma quartzite and schist (SM10-021 DZ; Fig. 2A) above the Neoproterozoic Lesser Himalayan Deoban and Mandhali Formations. Thus, the Berinag thrust again occupies a similar structural position as the Ramgarh-Munsiari thrust. In addition, the north, south, and central Chiplakot thrusts underlie the Chiplakot klippe and its Paleoproterozoic orthogneiss (Phukon et al., 2018) and may correlate with the Berinag thrust/Ramgarh-Munsiari thrust. North of the Chiplakot klippe, the Ramgarh-Munsiari thrust sheet, which roots into the immediate Main Central thrust footwall, consists of abundant Paleoproterozoic augen gneiss with a crystallization age of 1860 ± 19 Ma (sample SM11-048; Fig. 2A; also see Phukon et al., 2018), and metasedimentary rocks with large negative (-25.6) ϵ_{Nd} values (sample SM11-049; Fig. 2A). The consistency of Lesser Himalayan Paleoproterozoic metasedimentary and igneous rocks and very negative ϵ_{Nd} values (-20 to -25) suggests that the Berinag thrust is actually an isolated klippe of the Ramgarh-Munsiari thrust sheet.

Metamorphic conditions are consistent with these interpretations. Along strike to the west and east, Paleoproterozoic Munsiari Formation rocks in the Main Central thrust footwall are metamorphosed to amphibolite facies at pressure-temperature conditions of ~ 575 °C and ~ 8 kbar (Spencer et al., 2012a; Iaccarino et al., 2017). In contrast, beneath the Almora klippe, Paleoproterozoic Lesser Himalayan rocks are metamorphosed to greenschist-facies conditions (chlorite-biotite phyllite; Joshi and Tiwari, 2009 likely 400–500 °C (e.g., Ferry, 1984). The difference in temperatures from north to south results from the fact that the rocks carried by the Ramgarh-Munsiari thrust in the north were buried deeper than those to the south along a lateral thermal gradient, as has been inferred elsewhere in the Himalaya (Kohn, 2008).

Lesser Himalayan rocks carried by the Ramgarh-Munsiari thrust sheet are (1) granitoid plutons of arc affinity (Kohn et al., 2010; see also Miller et al., 2000) that formed during a major crustal reworking event at ca. 1850 (Mandal et al., 2016), and (2) ca. 1800 Ma metasedimentary rocks (clastic and volcanoclastic supracrustal rocks) from the Paleoproterozoic arc-assemblage (Kohn et al., 2010; Mandal et al., 2016) that blanketed the ca. 2500 old Indian cratonic basement (Mondal et al., 2002), at least in the Garhwal-Kumaun region. These plutonic and volcanic rocks of the

Paleoproterozoic arc postdate formation of ca. 2500 Ma cratonic India, so they cannot represent Indian basement as proposed by C  lerier et al. (2009). As a result of these data, we propose that the Askot and Chiplakot klippen are erosional remnants of an originally continuous Ramgarh-Munsiari thrust sheet that was emplaced over the top of Neoproterozoic–Cambrian Lesser Himalayan rocks.

Balanced Cross Section

Our balanced cross section shows that the structural geometry consists of a hinterland-dipping duplex system of Lesser Himalayan rocks, with the Main Central thrust and Ramgarh-Munsiari thrust acting as a coupled roof thrusts and the Main Himalayan thrust acting as a floor thrust (Fig. 7A), similar to far western and central Nepal (DeCelles et al., 2001; Robinson et al., 2006; Khanal and Robinson, 2013; Robinson and Martin, 2014) and in Bhutan (McQuarrie et al., 2008; Long et al., 2011). Based on similar lithologic assemblages and Paleoproterozoic ages of the thrust sheet rocks carried on the Munsiari thrust, Berinag thrust, Chiplakot klippe, Askot klippe, and Ramgarh thrust, we interpret these as all part of one folded, far-traveled thrust sheet, the Ramgarh-Munsiari thrust. The Ramgarh-Munsiari thrust and another thrust sheet structurally form the immediate footwall of the northernmost Main Central thrust (Fig. 7A). The Ramgarh-Munsiari thrust is folded, forming the klippen, commonly referred to as “Lesser Himalayan Crystallines” (e.g., Patel et al., 2011, and references therein). The Ramgarh-Munsiari thrust sheet, along with the North Almora thrust–South Almora thrust (i.e., Almora thrust/Main Central thrust) sheet, is regionally folded along a WNW-ESE-trending axis forming the Almora klippe (Fig. 7A). Near-parallel bedding (S_0) and foliation (S_1) dips of the Ramgarh-Munsiari thrust and Almora klippe rocks suggest a possible flat-on-flat relationship (Fig. 2A). Folding of the Ramgarh-Munsiari thrust and Main Central thrust sheets occurred as the Lesser Himalayan duplex formed.

The Lesser Himalayan duplex consists of seven north-dipping thrust sheets (A–G in Figs. 7A and 7B) with an average thickness of ~ 4700 m. The number of thrust sheets (i.e., horses) was determined based on surface dips, stratigraphic information, and available space between the northernmost exposure of the Ramgarh-Munsiari thrust and the Main Himalayan thrust ramp, defined from a common conversion point (CCP) image (Caldwell et al., 2013). All these thrust sheets contain rocks from the Ramgarh/Berinag/Munsiari Formations, Rautgara/Chakrata Formations, and Deoban/Mandhali Formations. Thrust sheet G additionally contains Neoproterozoic–Cambrian Lesser Himalayan rocks, including the Chandpur/Nagthat Formation and overlying strata. The thrust sheets in this hinterland-dipping system progressively steepen to the north. The Main Central thrust and Ramgarh-Munsiari thrust sheets were emplaced on top of undeformed Lesser Himalayan rocks. Formation of the Lesser Himalayan duplex deformed these thrust sheet rocks into a series of anticlines and synclines. The synclines preserve hanging-wall rocks of the Main Central thrust in the Almora klippe and of the Ramgarh-Munsiari thrust in the Chiplakot, Askot, and Almora klippen. Thrust sheets A–C lie in the proximal footwall of the northernmost exposure of the Ramgarh-Munsiari thrust. Thrust sheets B and C were buried beneath the Chiplakot klippe and are required to fill the space between exposed thrust sheets A and D. Thrust sheets D and E control the geometry of the asymmetrical Askot klippe, while thrust sheets F and G form two anticlines north of the Almora klippe. Emplacement of this hinterland-dipping duplex folded the Ramgarh-Munsiari thrust and overlying Main Central thrust sheets to form the Almora klippe. Thrust sheet G forms a broad fault-bend fold, which was subsequently cut by three out-of-sequence faults located immediately north of the northern limb of Almora syncline (Fig.

7A). These three faults have both normal and thrust motions and likely formed at different times in response to the super- and subcritical stages of the Himalayan wedge (e.g., Robinson, 2008). These faults breach the overlying Ramgarh-Munsiari thrust and Main Central thrust (Fig. 7A) and juxtapose the Paleoproterozoic Rautgara Formation against the Paleoproterozoic Ramgarh Formation (Fig. 7A). Thrust sheet F is also cut by one out-of-sequence fault. Growth of these out-of-sequence faults caused variability in the orientations of bedding and foliations north of the Almora klippe. The Ramgarh-Munsiari thrust sheet changes thickness from 3–4 km at its northernmost exposure in the footwall of the Main Central thrust to ~1 km in its southernmost exposure south of the Almora klippe (Fig. 7A) as the thrust cuts up through the Paleoproterozoic Lesser Himalayan rock in the transport direction.

The southernmost Lesser Himalayan thrust sheet dictates the structural geometry between the Ramgarh-Munsiari thrust of the Almora klippe to the north and the Main Boundary thrust to the south with a broad syncline and an out-of-sequence thrust. The broad syncline exposes the Neoproterozoic Nagthat Formation (ca. 560 Ma; Fig. 7A, annotation 12). The out-of-sequence thrust juxtaposes clean Paleoproterozoic quartzite with intercalated mafic schist of the Rautgara Formation against the Neoproterozoic micaceous quartzite of the Nagthat Formation. Emplacement of this thrust sheet likely folded the southern Almora klippe toward the north. In the Subhimalayan thrust system, the northernmost thrust sheet, the Main Dun thrust sheet, carries the north-dipping Lugad Gad Formation and overlies the younger lower Siwalik unit. South of the Main Dun thrust, the Main Frontal thrust lacks southerly dipping beds, indicating that the Main Frontal thrust hanging wall at present day preserves only the north-dipping limbs of eroded, hanging-wall anticlines (Fig. 7A).

Restoration of our balanced cross section into an undeformed geometry (Fig. 7B), including restoration of the deformed Tethyan Himalaya (Murphy and Yin, 2003), yields a minimum estimate of original length (L_0) of ~674–751 km on this cross section (Table 4). The deformed length (L_f) of the cross section is ~141 km (Fig. 7A). Hence, the total minimum amount of shortening ($L_0 - L_f$) by various structures between the Main Frontal thrust to the south and the Main Central thrust to the north ranges between ~541 km (79%) and ~575 km (80%). This reconstruction represents a minimum amount of shortening (~128 km) on the Main Central thrust if Greater Himalayan rocks were emplaced as a slab. If rocks of the Almora klippe were carried on another intra-Greater Himalayan thrust sheet, shortening amounts are greater (~163 km). Moreover, shortening must have been greater than we have calculated because we excluded penetrative strain, small-scale shortening structures, and intra-Greater

Himalayan thrust sheets (Montomoli et al., 2013, 2015; Larson et al., 2015; Braden et al., 2017). The Ramgarh-Munsiari thrust has minimum shortening of ~112 km, while the Lesser Himalayan duplex accommodates ~270 km of minimum shortening. The Subhimalayan thrust system has ~22 km of minimum shortening.

DISCUSSION

Lesser Himalayan Duplex Structural Geometry and Along-Strike Variability

Our balanced cross section-based structural geometry was derived by incorporating recent and new stratigraphic information, including the following: (1) The Almora klippe is not the southward continuation of the Paleoproterozoic Munsiari thrust sheet, but rather it contains Neoproterozoic–Ordovician Greater Himalaya affinity rocks; (2) the Munsiari, Berinag, and Ramgarh thrusts are part of a once-continuous thrust sheet of Paleoproterozoic rocks that was carried by the Ramgarh-Munsiari thrust sheet; (3) Ramgarh-Munsiari thrust sheet rocks are present on the either side of the Almora klippe, carrying only Paleoproterozoic rocks north of the Almora klippe, but both Paleoproterozoic and Neoproterozoic rocks south of the Almora klippe; and (4) ca. 1600 Ma Rautgara Formation rocks are present on the north side of Almora klippe, structurally below the Ramgarh-Munsiari thrust (Fig. 7A). These stratigraphic data require revision of the cross sections of Srivastava and Mitra (1994) and C  lerier et al. (2009). In such revisions, the location and dip amount of the midcrustal ramp in the Lesser Himalayan stratigraphy are crucial for determining the correct geometry of the Lesser Himalayan duplex. This geometry is known from new seismic reflection data ~125 km west of our study area, based on the positive impedance contrast due to juxtaposition of Ramgarh-Berinag-Munsiari (Paleoproterozoic Lesser Himalayan) rocks against the carbonate rocks of the Deoban and Mandhali Formations (Caldwell et al., 2013). These data provide more definitive geometries of the midcrustal ramp and require less extrapolation in comparison to previous studies. For example, the midcrustal Lesser Himalayan ramp in the Srivastava and Mitra (1994) cross section is 30 km north of the interpreted ramp in Caldwell et al. (2013). Given that the reflection profile that we used to determine the midcrustal ramp geometry of our cross section is ~125 km to the west, it is possible that lateral ramps shift the midcrustal Lesser Himalayan ramp slightly to the north or south compared to our cross sections.

Because the hinterland-dipping Lesser Himalayan duplex accommodates the most shortening (270 km or 40% of the total shortening; Table 4), it thereby controls the structural architecture of Kumaun. Although the Lesser Himalayan duplex is ubiquitous along strike throughout the Himalaya, geometries and participating rock units vary (Srivastava and Mitra, 1994; Robinson et al., 2006; Long et al., 2011; Khanal and Robinson, 2013; Webb, 2013; Bhattacharyya et al., 2015a; Robinson and Martin, 2014; Parui and Bhattacharyya, 2018) as follows:

(1) Himachal Pradesh (west of our study area): The hinterland-dipping Lesser Himalayan duplex contains Paleoproterozoic rocks to the north overlain by Neoproterozoic–Cambrian rocks (Webb, 2013).

(2) Western and central Nepal: The hinterland-dipping duplex contains Paleoproterozoic and Mesoproterozoic rocks as well as Gondwana sedimentary rocks and Miocene foreland basin rocks (Robinson et al., 2006; Khanal and Robinson, 2013; Robinson and Martin, 2014).

(3) Sikkim (India): The Lesser Himalayan duplex contains Paleoproterozoic hinterland-dipping duplexes in the north and south, and a duplex that carries Paleoproterozoic–Permian rocks, the overall orientation of which ranges from hinterland-dipping to antiformal stack to

TABLE 4. ESTIMATION OF SHORTENING ALONG THE CROSS-SECTION LINE

Structures	L_f (km)	L_0 (km)	Shortening (km)	Shortening (%)
Main Frontal thrust	8.3	15.8	7.5	47.2
Main Dun thrust	4.8	19.7	14.9	75.8
Main Boundary thrust	1.5	9.0	7.6	83.3
Ramgarh-Munsiari thrust	51.7	163.9	112.2	68.5
Lesser Himalayan duplex	59.7	329.8	270.1	81.9
Main Central thrust maximum*	15.2	178.4	163.2	91.5
Main Central thrust minimum†	15.9	143.5	128.4	89.4
Total minimum shortening	141.2	681.7	540.6	79.3
Total maximum shortening	141.2	716.6	575.4	80.3
Shortening in the Tethyan Himalaya	–	–	133–176	–
Total shortening	–	–	674–751	–

Note: Shortening = ($L_f - L_0$) and Shortening % = $[(L_f - L_0)/L_0] \times 100$.

*Maximum if Almora klippe and Greater Himalaya are separate thrust sheets and overlying Greater Himalaya extends to northern edge of the klippe (Khanal et al., 2015b).

†Minimum if Almora klippe is southern continuation of Greater Himalaya.

foreland-dipping (Bhattacharyya and Mitra, 2009; Bhattacharyya et al., 2015a; Parui and Bhattacharyya, 2018). The part of the duplex to the south remains blind in eastern Sikkim, and the geometry varies from hinterland-dipping to foreland-dipping orientation (Parui and Bhattacharyya, 2018).

(4) Bhutan (eastern Himalaya): In eastern Bhutan, a hinterland-dipping Lesser Himalayan duplex system includes both Paleoproterozoic units in the north and Neoproterozoic to Cambrian (?) units in the south (Long et al., 2011). In western Bhutan, the northern part of the Lesser Himalayan duplex is modeled as having hinterland- to foreland-dipping orientation (Long et al., 2011; McQuarrie et al., 2014).

Comparison of Shortening Estimates in Kumaun

The minimum shortening estimate between the Main Frontal thrust and Indus suture zone (i.e., cumulative shortening taken up by Subhimalayan, Lesser Himalayan, Greater Himalayan, and Tethyan Himalayan rocks) along the Pindari cross section of Srivastava and Mitra (1994), ~70 km west of our cross section, is ~687–754 km or 69%–72%, while our total estimate is ~674–751 km. Our estimated shortening between the Main Frontal thrust and South Tibetan Detachment system is 541–575 km (79%–80%), while shortening estimated by Srivastava and Mitra (1994) was 354–421 km (76%–79%; Table 4). It is striking that these two studies have similar estimated shortening percentages, which is a function of undeformed cross-section length, even though they contain different stratigraphic assumptions (cf. Robinson and Martin, 2014). For example, Srivastava and Mitra (1994) reinterpreted the Berinag thrust (Valdiya, 1980) as a normal fault that replaced the Berinag Formation above the Damtha Group. However, our new chronostratigraphy reveals that the Berinag Formation is older (youngest zircon ca. 1800 Ma; McKenzie et al., 2011; Mandal et al., 2015) than the Damtha Group (youngest zircon ca. 1600 Ma; Mandal et al., 2015), implying a thrust fault. Our new chronostratigraphy also places the Ramgarh, Munsiri, and Berinag Formation in the same unit and on the same thrust sheet. As in many other studies, our minimum shortening estimate of ~700 km in the fold-thrust belt represents only approximately one third of the total convergence estimated for the central part of the Himalaya (van Hinsbergen et al., 2011). Estimated minimum shortening across the Himalaya, from west to east, is given in Table 5, including shortening of the Subhimalayan, Lesser Himalayan, and Greater Himalayan rocks. Drastic variations in shortening estimates exist, ranging between 258 and 780 km, with the highest total minimum shortening estimates from western Nepal (691–780 km; Robinson et al., 2006). Such variations in minimum shortening estimates across the Himalayan fold-thrust belt are the result of differences in assumptions regarding ramp geometry and location, initial width of the precursor basin, and variations in lithologic/stratigraphic packages that control rock mechanics.

Temporal Evolution

The ages of deformation for the Tethyan Himalayan, Greater Himalayan, and Lesser Himalayan rocks were constrained using published U-Pb crystallization ages on zircon and monazite, and $^{40}\text{Ar}/^{39}\text{Ar}$ thermochronology on muscovite. Here, we emphasize results from Garhwal and far western Nepal, because these regions are proximal to Kumaun.

Tethyan Deformation and the South Tibetan System

Between ca. 55 and 25 Ma, Tethyan Himalayan rocks experienced thrusting and crustal thickening, leading to the burial and metamorphism of Greater Himalayan rocks (Harrison et al., 1997; Searle et al., 1999; Catlos et al., 2001; Godin et al., 2001; Kohn, 2008; Dunkl et al., 2011; Kohn, 2014; Braden et al., 2017; Montomoli et al., 2017). In Garhwal, ~95 km west of our Kumaun cross section, monazite ages constrain initial high-temperature cooling and crystallization of melts at ca. 25 Ma (see Iaccarino et al., 2017). These data suggest earliest movement on the South Tibetan Detachment system and consequently termination of Tethyan Himalaya thickening prior to 25 Ma. The Malari granite (Sachan et al., 2010) reflects decompressional melting of underlying Greater Himalayan rocks (Iaccarino et al., 2017), intrudes the South Tibetan Detachment system, and shows postemplacement brittle-ductile to brittle deformation (Sen et al., 2015). Zircon crystallization ages indicate that high-temperature ductile movement along the South Tibetan Detachment system ceased by ca. 19 Ma (Sachan et al., 2010). Muscovite $^{40}\text{Ar}/^{39}\text{Ar}$ cooling ages of 15.2 Ma from the Malari granite suggest that brittle-ductile deformation along the South Tibetan Detachment system may have continued until ca. 15 Ma (Sen et al., 2015; Iaccarino et al., 2017; Montemagni et al., 2019).

Greater Himalayan Deformation and the Main Central Thrust

In western Nepal, 230 km east of our Kumaun cross section, peak burial of Greater Himalayan rocks, presumably by the Tethyan thrust belt, occurred between 36 and 30 Ma (La Roche et al., 2016). Intra-Greater Himalayan faults have been found north of the Main Central thrust that moved between 28 and 17 Ma (Montomoli et al., 2013, 2015; Carosi et al., 2016; 2018). In the same region, shearing along the South Tibetan Detachment system ended between 25 and 23 Ma (Carosi et al., 2013). Intra-Greater Himalayan faults have not been reported yet in Kumaun and Garhwal, but their widespread occurrence along strike suggests they are likely present. The age of the Main Central thrust is reported as between 16 and 9 Ma in Garhwal (Montemagni et al., 2018), but it is as yet unknown in Kumaun. Muscovite $^{40}\text{Ar}/^{39}\text{Ar}$ cooling ages from the immediate Main Central thrust hanging wall in far western Nepal were interpreted to indicate an age of motion on the Main Central thrust at ca. 25 Ma; however, the spectra are disturbed, and the age is likely ≤ 20 Ma (fig. 11 of Robinson et al., 2006). North of the easternmost part of the Dadeldhura klippe, motion

TABLE 5. ESTIMATION OF SHORTENING ALONG THE CROSS-SECTION LINE

Location	SH + LH in km (%)	SH + LH + GH in km (%)	References
Pakistan	—	470 (64%)	Coward and Butler (1985)
Himachal Pradesh, India	—	518 (72%)	Webb (2013)
Kumaun-Garhwal, India	161 (65%)	354–421 (76%–79%)	Srivastava and Mitra (1994)
Kumaun, India	412 (76%)	541–575 (79%–80%)	This study
Western Nepal	393 (77%)	691–780 (79%–84%)	Robinson et al. (2006)
Central Nepal	284 (53%)	400 (75%)	Khanal and Robinson (2013)
Central Nepal	220–243 (71%–73%)	258–349 (69%–76%)	Robinson and Martin (2014)
Sikkim	253 (76%)	450 (81%)	Bhattacharyya et al. (2015a)
Sikkim	292	403 (80%)	Parui and Bhattacharyya (2018)
Bhutan	164–267 (52%–66%)	302–476 (70%–75%)	Long et al. (2011)

Note: SH—Subhimalaya; LH—Lesser Himalaya; GH—Greater Himalaya.

on the Main Central thrust occurred between 18 and 13 Ma (Montomoli et al., 2013; Iaccarino et al., 2017). A younger muscovite $^{40}\text{Ar}/^{39}\text{Ar}$ cooling age in Garhwal could imply an age for motion on the Main Central thrust as young as 6.3 Ma. However, young cooling ages north of the Main Central thrust are common along the Himalayan arc due to uplift and exhumation from a ramp in the Main Himalayan thrust (McQuarrie and Ehlers, 2015, 2017; Gilmore et al., 2018).

In far western Nepal, the eastern extension of the Almora klippe is the Dadeldhura klippe. Greater Himalayan rocks within the Dadeldhura klippe cooled through the muscovite $^{40}\text{Ar}/^{39}\text{Ar}$ closure temperature (nominally 400–425 °C; Harrison et al., 2009) at 22.7 Ma on the southern margin of the klippe, 21 Ma toward the klippe center, and 18.2 Ma on the northern margin (Robinson et al., 2006; Antolin et al., 2013). An emplacement age of 23–18 Ma for the combined Dadeldhura-Almora klippe is supported by zircon fission-track data from Singh and Patel (2017) that range in age from 21 Ma on the south side to 13 Ma on the north side of the klippe. Zircon fission-track ages have a closure temperature of 260 °C with a partial retention zone between 260 °C and 200 °C (Peyton and Carrapa, 2013), so ages that are younger than the muscovite cooling ages are expected. If the Almora-Dadeldhura klippe was emplaced between 23 and 18 Ma, and motion on the Main Central thrust was not until 18–13 Ma, the Greater Himalayan klippe rocks may have been emplaced by intra-Greater Himalayan thrusts as suggested by Khanal et al. (2015b) in central Nepal.

Ramgarh-Munsiari Thrust

In far western Nepal, Robinson et al. (2006) estimated motion on the Ramgarh-Munsiari thrust to be between ca. 17 and 10 Ma, based on muscovite $^{40}\text{Ar}/^{39}\text{Ar}$ cooling ages. Initial movement of the Ramgarh-Munsiari thrust must have occurred at 16 ± 1 Ma because the thrust cuts the ca. 15 Ma Dumri Formation (DeCelles et al., 2001). In Kumaun, C  lerier et al. (2009b) reported muscovite $^{40}\text{Ar}/^{39}\text{Ar}$ cooling ages of 13.6–9.8 Ma from the Askot klippe, part of the Ramgarh-Munsiari thrust sheet. Bollinger et al. (2006) in far western Nepal, 45 km east of our study area, reported a hornblende $^{40}\text{Ar}/^{39}\text{Ar}$ cooling age of 13 ± 2 Ma and low-temperature (<370 °C) retrograde monazite at ca. 10 and 4 Ma. If motion on the Main Central thrust halted between 17 and 13 Ma, the Ramgarh-Munsiari thrust motion must have begun afterward. Paleoproterozoic detritus from this sheet eroding and collecting in the Siwalik Group is ca. 11–10 Ma in far western Nepal (Robinson and McQuarrie, 2012). Based on the data, perhaps an age of motion on the Ramgarh-Munsiari thrust is 14–10 Ma.

Lesser Himalayan Duplex

The Lesser Himalayan duplex may have started to form at ca. 10 Ma in western Nepal (Robinson et al., 2001, 2006), and perhaps also in Kumaun. In regions that are located near our study area but outside of Figure 2, Lesser Himalayan rock temperatures decrease from ~550 °C in the Ramgarh-Munsiari thrust (Spencer et al., 2012b, from Garhwal) to <330 °C in southern part of the Lesser Himalayan duplex (C  lerier et al., 2009). The last thrust in the Lesser Himalayan duplex is the Main Boundary thrust, and it has no timing constraints in Kumaun. In central Nepal, motion on the Main Boundary thrust cuts the lower part of the upper Siwalik unit, limiting first motion to ca. 4 Ma (Ojha et al., 2008). Although there are no data in Kumaun, a general age for the timing of the Subhimalayan thrust system is from mid-Pliocene to present (Wesnousky et al., 1999; Lav   and Avouac, 2000).

Kinematic Evolution

Our new structural geometric model differs significantly from previous interpretations (Srivastava and Mitra, 1994; C  lerier et al., 2009),

and in combination with the new timing data presented herein, it warrants a new kinematic model explaining the structural evolution along the cross-section line. This model begins with the assumption that the Lesser Himalayan rocks represent passive-margin sediments that blanketed the pre-Himalayan, northern Indian cratonic margin (Fig. 8A; e.g., Rupke, 1974; Valdiya, 1980; Brookfield, 1993; Ahmad et al., 2000; Miller et al., 2000; DeCelles et al., 2001; Myrow et al., 2003, 2010; Richards et al., 2005; Mandal et al., 2016). Tethyan Himalayan and some Lesser Himalayan rocks are Paleozoic to Cretaceous in age, and we assume they were deposited horizontally atop the Paleoproterozoic–Neoproterozoic Lesser Himalayan rocks. Because there is no record of pre-Tertiary deformation and metamorphism in India (C  lerier et al., 2009; Kohn et al., 2010), we assume these Lesser Himalayan rocks were also flat-lying strata. This initial configuration (Fig. 8A) precedes the earliest reported deformation and metamorphism (ca. 40 Ma), before formation of any Greater Himalaya tectono-metamorphic discontinuities (see Carosi et al., 2018). In addition, the northern termination of Lesser Himalayan rocks is unknown, so the length of the Lesser Himalayan strata could have been much greater than the minimum shown in Figure 8A. The location of Greater Himalayan rocks in relationship to Lesser Himalayan rocks is also unknown, but Greater Himalayan rocks come from a midcrustal location deeper than the Lesser Himalayan rocks and must have originated further north than Lesser Himalayan rocks. To minimize shortening, we assume that the North and South Almora thrust is the same thrust as the Main Central thrust, although the klippe could be an intra-Greater Himalayan thrust sheet (e.g., Cottle et al., 2015; Khanal et al., 2015b; Wang et al., 2015; Parsons et al., 2016).

Because intra-Greater Himalaya thrusting has not yet been identified in Kumaun, Figure 8B begins with motion on the Main Central thrust. If the Dadeldhura-Almora klippe was emplaced by an intra-Greater Himalayan fault, the age for that would be ca. 23–18 Ma. If, as is shown in Figure 8B for simplification, the Main Central thrust emplaced the klippe, the timing of motion would likely be 17–13 Ma (Montomoli et al., 2013). Following motion on the Main Central thrust, the Ramgarh-Munsiari thrust imbricate sheet and the Ramgarh-Munsiari thrust incorporated Lesser Himalayan rocks into the wedge and were emplaced over other Lesser Himalayan rocks that would become the Lesser Himalayan duplex (Fig. 8C). Movement on the main part of the Ramgarh-Munsiari thrust must have initiated after 17 Ma (Carosi et al., 2018). Given the data in the Garhwal–western Nepal region, we suggest an age of ca. 14–10 Ma for the Ramgarh-Munsiari thrust imbricate sheet and the Ramgarh-Munsiari thrust.

From ca. 10 to 4 Ma, thrust sheets A–G were emplaced from hinterland to foreland, with the Main Boundary thrust as the last thrust sheet in the system (Figs. 8D–8F). The overlying Ramgarh-Munsiari thrust and Main Central thrust sheets were passively translated southward and folded as the Lesser Himalayan duplex grew. Growth of the Lesser Himalayan duplex folded the northern part of the Almora klippe to dip southward. Apatite fission-track ages indicate that this folding occurred sometime between 13 and 7 Ma (Patel et al., 2015). Folding of the southern edge of the Almora klippe and underlying Ramgarh-Munsiari thrust may have occurred as the Main Boundary thrust was emplaced. In central Nepal, the age for the Main Boundary thrust is ca. 4 Ma (Ojha et al., 2008); however, apatite fission-track cooling ages are 7–6 Ma in the Ramgarh-Munsiari thrust sheet (Patel et al., 2015), which was folded along with the klippe rocks in the southern part of the Almora klippe. These observations indicate that first motion on the Main Boundary thrust in Kumaun may have started earlier (>7–6 Ma) than in central Nepal. Motion on the Subhimalayan thrust system brings the fold-thrust belt to a nearly complete configuration (Fig. 8G).

Our final deformation frame (Fig. 8H) takes into account out-of-sequence faults, which commonly form in thrust belts as a wedge readjusts to critical taper by either building taper (thrust faults) or reducing

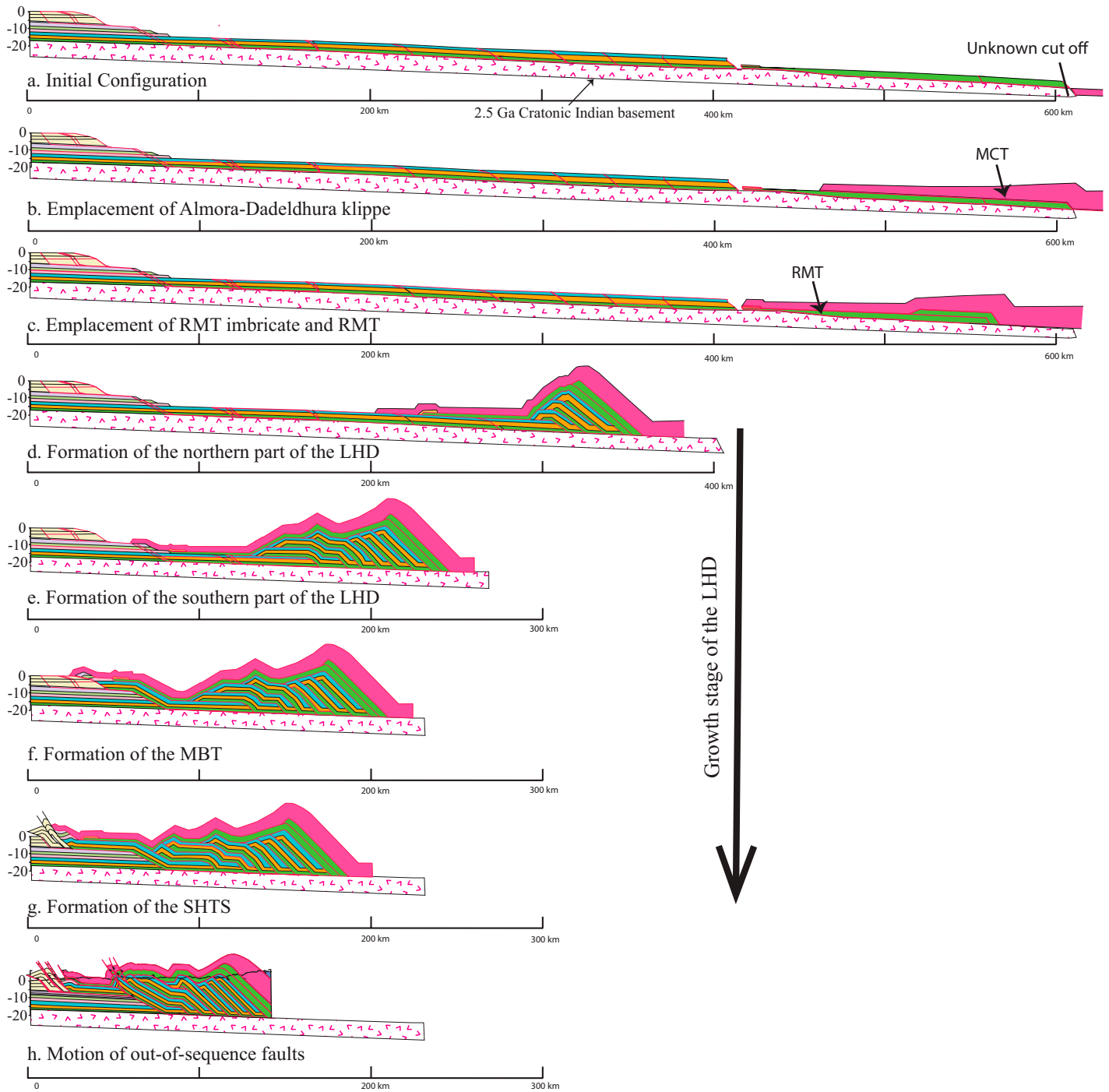


Figure 8. Reconstruction along the cross-section line in Figure 2A. In each time frame, fault(s) that will be moved in the next time frame are shown in the undeformed stratigraphy. Unit colors are the same as Figure 7. LHD—Lesser Himalayan duplex; MBT—Main Boundary thrust; MCT—Main Central thrust; RMT—Ramgarh-Munsiari thrust; SHTS—Subhimalayan thrust system.

taper (normal faults; e.g., Davis et al., 1983). In kinematic models, the point at which these faults are imposed does not affect large-scale interpretations; this is why we impose them after thickening of the orogenic wedge. However, including these faults does more accurately reflect field relationships and our final cross section. Out-of-sequence thrusting at the northern edge of the Almora klippe may be linked with the growth of the out-of-sequence thrust systems in thrust sheet G, tilting the northern part of the Almora klippe (Fig. 8G). In Kumaun, a series of in-sequence thrusts dominated formation of the orogenic wedge from early Miocene time to the present; thus, most of the evolution the Himalayan fold-thrust belt can be simply explained as a critically tapered wedge.

CONCLUSIONS

We present a new mapping and structural interpretation based on our revised chronostratigraphy in Kumaun, northwest India, and find the following main points:

(1) The Ramgarh, Berinag, and Munsiri rocks, including Paleoproterozoic gneiss, were part of a once-continuous Paleoproterozoic unit that was translated south on the Ramgarh-Munsiri thrust. Growth of the underlying Lesser Himalayan duplex folded the thrust sheet, and erosion isolated thrust sheets into synclinal klippen.

(2) The Almora thrust sheet (= Main Central thrust) and the underlying Ramgarh-Munsiri thrust sheet together formed the coupled roof thrust system for the Lesser Himalayan duplex. Progressive growth of the Lesser Himalayan duplex folded the overlying thrust sheets and shaped the final geometry of the Almora klippe.

(3) The Himalayan fold-thrust belt in Kumaun is a forward-propagating thrust system, typical of thin-skinned-style tectonics.

(4) The Lesser Himalayan duplex has accommodated ~270 km of minimum shortening. We estimate a total minimum shortening from the Main Frontal thrust to the South Tibetan Detachment system of ~541–575 km. By adding shortening in the Tethyan Himalaya, we calculate a total minimum shortening between ~674 and 751 km in Kumaun.

(5) The revised stratigraphy-based balanced cross section increases the previously estimated shortening in the Greater, Lesser, and Subhimalayan rocks by ~120–200 km.

ACKNOWLEDGMENTS

This project was funded by the National Science Foundation (NSF grants EAR-0809405, to Robinson, and EAR-0809428, EAR-1048124, and EAR-1321897 to Kohn). Mandal thanks the Graduate School and the Department of Geological Sciences at the University of Alabama for travel support to carry out the field work and U-Pb zircon geochronologic analyses. Mark Pecha, Nicky Giesler, and Mauricio Ibanez are thanked for their help during U-Pb analysis at the Arizona LaserChron Center (NSF grant EAR-1032156). We also thank Jeff Vervoort, Washington State University, for performing the whole-rock Nd analysis. This manuscript greatly benefited from careful reviews by two anonymous reviewers, as well as editorial handling by Damian Nance.

REFERENCES CITED

Ahmad, T., Harris, N., Bickel, M., Chapman, H., Bunbury, J., and Prince, C., 2000, Isotopic constraints on the structural relationships between the Lesser Himalayan Series and the High Himalayan Crystalline Series, Garhwal Himalaya: *Geological Society of America Bulletin*, v. 112, no. 3, p. 467–477, [https://doi.org/10.1130/0016-7606\(2000\)112<467:ICOTSR>2.0.CO;2](https://doi.org/10.1130/0016-7606(2000)112<467:ICOTSR>2.0.CO;2).

Antolin, B., Godin, L., Wemmer, K., and Nagy, C., 2013, Kinematics of the Dadelhdura klippe shear zone (western Nepal): Implications for the forward evolution of the Himalayan metamorphic core: *Terra Nova*, v. 25, p. 282–291, <https://doi.org/10.1111/ter.12034>.

Avouac, J., 2003, Mountain building, erosion, and the seismic cycle in the Nepal Himalaya, *in* Dmowska, R., ed., *Advances in Geophysics* Volume 46: Amsterdam, Netherlands, Elsevier, p. 1–80.

Avouac, J.P., 2015, Mountain building: From earthquakes to geologic deformation, *in* Watts, A.B., ed., *Crust and Lithosphere Dynamics: Treatise on Geophysics*, Volume 6: Oxford, UK Elsevier, p. 381–432.

Beaumont, C., and Jamieson, R.A., 2010, Himalayan-Tibetan Orogeny: Channel Flow versus (critical) Wedge Models, A False Dichotomy?: U.S. Geological Survey Open-File Report 2010–1099, <http://pubs.usgs.gov/of/2010/1099/beamont/>.

Beaumont, C., Jamieson, R.A., Nguyen, M.H., and Lee, B., 2001, Himalayan tectonics explained by extrusion of a low-viscosity crustal channel coupled to focused surface denudation: *Nature*, v. 414, p. 738–742, <https://doi.org/10.1038/414738a>.

Beaumont, C., Jamieson, R.A., Nguyen, M.H., and Medvedev, S., 2004, Crustal channel flows: 1. Numerical models with applications to the tectonics of the Himalayan-Tibetan orogen: *Journal of Geophysical Research*, v. 109, B06406, <https://doi.org/10.1029/2003JB002809>.

Bhattacharyya, K., and Mitra, G., 2009, A new kinematic evolutionary model for the growth of a duplex—An example from the Rangit duplex, Sikkim Himalaya, India: *Gondwana Research*, v. 16, p. 697–715, <https://doi.org/10.1016/j.gr.2009.07.006>.

Bhattacharyya, K., Mitra, G., and Kwon, S., 2015a, Geometry and kinematics of the Darjeeling–Sikkim Himalaya, India: Implications for the evolution of the Himalayan fold-thrust belt: *Journal of Asian Earth Sciences*, v. 113, p. 778–796, <https://doi.org/10.1016/j.jseas.2015.09.008>.

Bhattacharyya, K., Dwivedi, H.V., Das, J.P., and Damania, S., 2015b, Structural geometry, microstructural and strain analyses of L-tectonites from Paleoproterozoic orthogneiss: Insights into local transport-parallel constrictional strain in the Sikkim Himalayan fold thrust belt: *Journal of Asian Earth Sciences*, v. 107, p. 212–231, <https://doi.org/10.1016/j.jseas.2015.04.038>.

Boelrijk, N.A.I.M., 1968, A general formula for “double” isotope dilution analysis: *Chemical Geology*, v. 3, no. 4, p. 323–325.

Bollinger, L., Henry, P., and Avouac, J., 2006, Mountain building in the Nepal Himalaya: Thermal and kinematic model: *Earth and Planetary Science Letters*, v. 244, p. 58–71, <https://doi.org/10.1016/j.epsl.2006.01.045>.

Braden, Z., Godin, L., and Cottle, J.M., 2017, Segmentation and rejuvenation of the Greater Himalayan sequence in western Nepal revealed by in situ U-Th/Pb monazite petrochronology: *Lithos*, v. 284, p. 751–765, <https://doi.org/10.1016/j.lithos.2017.04.023>.

Brookfield, M.E., 1993, The Himalayan passive margin from Precambrian to Cretaceous times: *Sedimentary Geology*, v. 84, no. 1–4, p. 1–35.

Burchfiel, B.C., and Royden, L.H., 1985, North-south extension within the convergent Himalayan region: *Geology*, v. 13, p. 679–682, [https://doi.org/10.1130/0091-7613\(1985\)13<679:NEWTCH>2.0.CO;2](https://doi.org/10.1130/0091-7613(1985)13<679:NEWTCH>2.0.CO;2).

Burchfiel, B.C., Zhihang, C., Hodges, K.V., Yuping, L., Royden, L.H., and Changrong, D., 1992, The South Tibetan Detachment System, Himalayan Orogen: Extension Contemporaneous With and Parallel To Shortening in a Collisional Mountain Belt: *Geological Society of America Special Paper* 269, 41 p., <https://doi.org/10.1130/SPE269-p1>.

Caldwell, W.B., Klempner, S.L., Lawrence, J.F., and Ashish, S.S.R., 2013, Characterizing the Main Himalayan thrust in the Garhwal Himalaya, India, with receiver function CCP stacking: *Earth and Planetary Science Letters*, v. 367, p. 15–27, <https://doi.org/10.1016/j.epsl.2013.02.009>.

Carosi, R., Montomoli, C., Rubatto, D., and Visonà, D., 2013, Leucogranite intruding the South Tibetan detachment in western Nepal: Implications for exhumation models in the Himalayas: *Terra Nova*, v. 25, p. 478–489, <https://doi.org/10.1111/ter.12062>.

Carosi, R., Montomoli, C., Iaccarino, S., Massonne, H.J., Rubatto, D., Langone, A., Gemignani, L., and Visonà, D., 2016, Middle to late Eocene exhumation of the Greater Himalayan Sequence in the Central Himalayas: Progressive accretion from the Indian plate: *Geological Society of America Bulletin*, v. 128, p. 1571–1592, <https://doi.org/10.1130/B31471.1>.

Carosi, R., Montomoli, C., and Iaccarino, S., 2018, 20 years of geological mapping of the metamorphic core across Central and Eastern Himalayas: *Earth-Science Reviews*, v. 177, p. 124–138, <https://doi.org/10.1016/j.earscirev.2017.11.006>.

Catlos, E.J., Harrison, T.M., Kohn, M.J., Grove, M., Ryerson, F.J., Manning, C.E., and Upreti, B.N., 2001, Geochronologic and thermobarometric constraints on the evolution of the Main Central Thrust, central Nepal Himalaya: *Journal of Geophysical Research: Solid Earth*, v. 106, B8, p. 16,177–16,204.

Célérier, J., Harrison, T.M., Webb, A.A.G., and Yin, A., 2009, The Kumaun and Garhwal Lesser Himalaya, India: Part 1. Structure and stratigraphy: *Geological Society of America Bulletin*, v. 121, p. 1262–1280, <https://doi.org/10.1130/B26344.1>.

Clift, P.D., 2006, Controls on the erosion of Cenozoic Asia and the flux of clastic sediment to the ocean: *Earth and Planetary Science Letters*, v. 241, no. 3–4, p. 571–580, <https://doi.org/10.1016/j.epsl.2005.11.028>.

Colchen, M., LeFort, P., and Pêcher, A., 1986, Geological Research in the Nepal Himalayas, Annapurna-Mansalu-Ganesh Himal: Paris, Centre National de la Recherche Scientifique, scale 1:20,000, 137 p.

Corrie, S.L., and Kohn, M.J., 2011, Metamorphic history of the central Himalaya, Annapurna region, Nepal, and implications for tectonic models: *Geological Society of America Bulletin*, v. 123, p. 1863–1879, <https://doi.org/10.1130/B30376.1>.

Cottle, J.M., Larson, K.P., and Kellelt, D.A., 2015, How does the mid-crust accommodate deformation in large, hot collisional orogens? A review of recent research in the Himalayan orogen: *Journal of Structural Geology*, v. 78, p. 119–133, <https://doi.org/10.1016/j.jsg.2015.06.008>.

Coward, M., and Butler, R.W.H., 1985, Thrust tectonics and the deep structure of the Pakistan Himalaya: *Geology*, v. 13, p. 417–420, [https://doi.org/10.1130/0091-7613\(1985\)13<417:TTATDS>2.0.CO;2](https://doi.org/10.1130/0091-7613(1985)13<417:TTATDS>2.0.CO;2).

Dahlen, F.A., 1990, Critical taper model of fold-and-thrust belts and accretionary wedges: *Annual Review of Earth and Planetary Sciences*, v. 18, p. 55–99, <https://doi.org/10.1146/annurev.ea.18.050190.000415>.

Dahlstrom, C.D.A., 1969, Balanced cross-sections: *Canadian Journal of Earth Sciences*, v. 6, p. 743–757, <https://doi.org/10.1139/e69-069>.

Das, J.P., Bhattacharyya, K., Mookerjee, M., and Ghosh, P., 2016, Kinematic analyses of orogen-parallel L-tectonites from Pelling-Munsiri area of Sikkim Himalayan fold thrust belt: Insights from multiple, incremental strain markers: *Journal of Structural Geology*, v. 90, p. 61–75, <https://doi.org/10.1016/j.jsg.2016.07.005>.

Davis, D., Suppe, J., and Dahlen, F.A., 1983, Mechanics of fold-and-thrust belts and accretionary wedges: *Journal of Geophysical Research*, v. 88, no. B2, p. 1153–1178, <https://doi.org/10.1029/JB088iB02p1153>.

- DeCelles, P.G., Gehrels, G.E., Quade, J., Ojha, T., Kapp, A., and Upreti, B.N., 1998, Neogene foreland basin deposits, erosional unroofing, and the kinematic history of the Himalayan fold-thrust belt, western Nepal: *Geological Society of America Bulletin*, v. 110, p. 2–21, [https://doi.org/10.1130/0016-7606\(1998\)110<0002:NFBDEU>2.3.CO;2](https://doi.org/10.1130/0016-7606(1998)110<0002:NFBDEU>2.3.CO;2).
- DeCelles, P.G., Gehrels, G.E., Quade, J., Lareau, B., and Spurlin, M., 2000, Tectonic implications of U-Pb zircon ages of the Himalayan orogenic belt in Nepal: *Science*, v. 288, p. 497–499, <https://doi.org/10.1126/science.288.5465.497>.
- DeCelles, P.G., Robinson, D.M., Quade, J., Copeland, P., Upreti, B.N., Ojha, T., and Garzzone, C.N., 2001, Regional structure and stratigraphy of the Himalayan fold-thrust belt, far western Nepal: *Tectonics*, v. 20, p. 487–509, <https://doi.org/10.1029/2000TC001226>.
- DeCelles, P.G., Robinson, D.M., and Zandt, G., 2002, Implications of shortening in the Himalayan fold-thrust belt for uplift of the Tibetan Plateau: *Tectonics*, v. 21, no. 6, p. 1062–1087, <https://doi.org/10.1029/2001TC001322>.
- DeCelles, P.G., Carrapa, B., Gehrels, G.E., Chakraborty, T., and Ghosh, P., 2016, Along-strike continuity of structure, stratigraphy, and kinematic history in the Himalayan thrust belt: The view from northeastern India: *Tectonics*, v. 35, no. 12, p. 2995–3027, <https://doi.org/10.1002/2016TC004298>.
- Dunkl, I., Antolin, B., Wemmer, K., Rantitsch, G., Kienast, M., Montomoli, C., Ding, L., Carosi, R., Appel, E., El Bay, R., and Xu, Q., 2011, Metamorphic evolution of the Tethyan Himalayan flysch in SE Tibet, in *Glaouen, R., and Ratschbacher, L., eds., Growth and Collapse of the Tibetan Plateau: Geological Society [London] Special Publication 353*, p. 45–69, <https://doi.org/10.1144/SP353.4>.
- Elliott, J.R., Jolivet, R., González, P.J., Avouac, J.P., Hollingsworth, J., Searle, M.P. and Stevens, V.L., 2016, Himalayan megathrust geometry and relation to topography revealed by the Gorkha earthquake: *Nature Geoscience*, v. 9, no. 2, p. 174, <https://doi.org/10.1038/NNGEO2623>.
- Ferry, J.M., 1984, A biotite isograd in south-central Maine, USA: mineral reactions, fluid transfer, and heat transfer: *Journal of Petrology*, v. 25, no. 4, p. 871–893.
- Gansser, A., 1964, *Geology of the Himalayas*: London, Wiley Interscience, 289 p.
- Gehrels, G.E., DeCelles, P.G., Ojha, T.P., and Upreti, B.N., 2006, Geologic and U-Pb geochronologic evidence for early Palaeozoic tectonism in the Dadelhdura thrust sheet, far-west Nepal Himalaya: *Journal of Asian Earth Sciences*, v. 28, p. 385–408, <https://doi.org/10.1016/j.jseae.2005.09.012>.
- Gehrels, G.E., Valencia, V.A., and Ruiz, J., 2008, Enhanced precision, accuracy, efficiency, and spatial resolution of U-Pb ages by laser ablation–multicollector–inductively coupled plasma–mass spectrometry: *Geochemistry Geophysics Geosystems*, v. 9, Q03017, <https://doi.org/10.1029/2007GC001805>.
- Gehrels, G., Kapp, P., DeCelles, P., Pullen, A., Blakey, L., Weislogel, A., Ding, A., Guynn, J., Martin, A., McQuarrie, N., and Yin, A., 2011, Detrital zircon geochronology of pre-Tertiary strata in the Tibetan-Himalayan orogen: *Tectonics*, v. 30, TC5016, <https://doi.org/10.1029/2011TC002868>.
- Gilmore, M.E., McQuarrie, N., Eizenhöfer, P.R., and Ehlers, T.A., 2018, Testing the effects of topography, geometry, and kinematics on modeled thermochronometer cooling ages in the eastern Bhutan Himalaya: *Solid Earth*, v. 9, p. 599–627, <https://doi.org/10.5194/se-9-599-2018>.
- Godin, L., and Harris, L.B., 2014, Tracking basement cross-strike discontinuities in the Indian crust beneath the Himalayan orogen using gravity data–relationship to upper crustal faults: *Geophysical Journal International*, v. 198, p. 198–215, <https://doi.org/10.1093/gji/ggu131>.
- Godin, L., Parrish, R.R., Brown, R.L., and Hodges, K.V., 2001, Crustal thickening leading to exhumation of the Himalayan metamorphic core of central Nepal: Insight from U-Pb geochronology and ⁴⁰Ar/³⁹Ar thermochronology: *Tectonics*, v. 20, no. 5, p. 729–747.
- Grandin, R., Vallée, M., Satriano, C., Lacassin, R., Klinger, Y., Simoes, M., and Bollinger, L., 2015, Rupture process of the Mw=7.9 2015 Gorkha earthquake (Nepal): Insights into Himalayan megathrust segmentation: *Geophysical Research Letters*, v. 42, no. 20, p. 8373–8382, <https://doi.org/10.1002/2015GL066044>.
- Grujic, D., Casey, M., Davidson, C., Hollister, L.S., Kündig, R., Pavlis, T., and Schmid, S., 1996, Ductile extrusion of the Higher Himalayan Crystalline in Bhutan: Evidence from quartz microfabrics: *Tectonophysics*, v. 260, p. 21–43, [https://doi.org/10.1016/0040-1951\(96\)00074-1](https://doi.org/10.1016/0040-1951(96)00074-1).
- Harrison, T.M., Copeland, P., Hall, S.A., Quade, J., Burner, S., Ojha, T., and Kidd, W.S.F., 1993, Isotopic preservation of Himalayan/Tibetan uplift, denudation, and climatic histories of two molasse deposits: *The Journal of Geology*, v. 101, p. 157–175, <https://doi.org/10.1086/648214>.
- Harrison, T.M., Célérier, J., Aikman, A.B., Hermann, J., and Heizler, M.T., 2009, Diffusion of ⁴⁰Ar in muscovite: *Geochimica et Cosmochimica Acta*, v. 73, p. 1039–1051, <https://doi.org/10.1016/j.gca.2008.09.038>.
- He, D., Webb, A.A.G., Larson, K.P., Martin, A.J., and Schmitt, A.K., 2015, Extrusion vs. duplexing models of Himalayan mountain building 3: Duplexing dominates from the Oligocene to present: *International Geology Review*, v. 57, p. 1–27, <https://doi.org/10.1080/00206814.2014.986669>.
- He, D., Webb, A.A.G., Larson, K.P., and Schmitt, A.K., 2016, Extrusion vs. duplexing models of Himalayan mountain building 2: The South Tibet detachment at the Dadelhdura klippe: *Tectonophysics*, v. 667, p. 87–107, <https://doi.org/10.1016/j.tecto.2015.11.014>.
- Heim, A., and Gansser, A., 1939, *Central Himalaya: Geological Observations of the Swiss Expedition 1936: Memoir of Swiss Society of Natural Science* 73, 245 p.
- Iaccarino, S., Montomoli, C., Carosi, R., Montemagni, C., Massonne, H.J., Langone, A., Jain, A.K., and Visonà, D., 2017, Pressure-temperature-deformation-time constraints on the South Tibetan detachment system in the Garhwal Himalaya (NW India): *Tectonics*, v. 36, p. 2281–2304, <https://doi.org/10.1002/2017TC004566>.
- Jain, A.K., Lal, N., Sulemani, B., Awasthi, A.K., Singh, S., Kumar, R., and Kumar, D., 2009, Detrital-zircon fission-track ages from the Lower Cenozoic sediments, NW Himalayan foreland basin: Cues for exhumation and denudation of the Himalaya during the India-Asia collision: *Geological Society of America Bulletin*, v. 121, p. 519–535, <https://doi.org/10.1130/B26304.1>.
- Jamieson, R.A., and Beaumont, C., 2013, On the origin of orogens: *Geological Society of America Bulletin*, v. 125, p. 1671–1702, <https://doi.org/10.1130/B30855.1>.
- Joshi, M., and Tiwari, A.N., 2009, Structural events and metamorphic consequences in Al-mora Nappe, during Himalayan collision tectonics: *Journal of Asian Earth Sciences*, v. 34, no. 3, p. 326–335.
- Karunakaran, C., and Rao, A.R., 1979, Status of Exploration for Hydrocarbons in the Himalayan Region—Contribution to Stratigraphy and Structure: *Geological Survey of India Miscellaneous Publication* 41, 66 p.
- Khanal, S., and Robinson, D.M., 2013, Upper crustal shortening and forward modeling of the Himalayan thrust belt along the Budhi-Gandaki River, central Nepal: *International Journal of Earth Sciences*, v. 102, p. 1871–1891, <https://doi.org/10.1007/s00531-013-0889-1>.
- Khanal, S., Robinson, D.M., Mandal, S., and Simkhada, P., 2015a, Structural, geochronological and geochemical evidence for two distinct thrust sheets in the ‘Main Central thrust zone’, the Main Central thrust and Ramgarh–Munsiari thrust: Implications for upper crustal shortening in central Nepal, in *Mukherjee, S., Carosi, R., van der Beek, P.A., Mukherjee, B.K., and Robinson, D.M., eds., Tectonics of the Himalaya: Geological Society [London] Special Publication 412*, p. 221–245, <https://doi.org/10.1144/SP412.2>.
- Khanal, S., Robinson, D.M., Kohn, M.J., and Mandal, S., 2015b, Evidence for a far-traveled thrust sheet in the Greater Himalayan thrust system, and an alternative model to building the Himalaya: *Tectonics*, v. 34, p. 31–52, <https://doi.org/10.1002/2014TC003616>.
- Kohn, M.J., 2008, P-T-t data from central Nepal support critical taper and repudiate large-scale channel flow of the Greater Himalayan sequence: *Geological Society of America Bulletin*, v. 120, p. 259–273, <https://doi.org/10.1130/B26252.1>.
- Kohn, M.J., 2014, Himalayan metamorphism and its tectonic implications: *Annual Review of Earth and Planetary Sciences*, v. 42, p. 381–419, <https://doi.org/10.1146/annurev-earth-060313-055005>.
- Kohn, M.J., Paul, S.K., and Corrie, S.L., 2010, The lower Lesser Himalayan sequence: A Paleoproterozoic arc on the northern margin of the Indian plate: *Geological Society of America Bulletin*, v. 122, p. 323–335, <https://doi.org/10.1130/B26587.1>.
- Kumar, R., Sangode, S.J., and Ghosh, S.K., 2004, A multistorey sandstone complex in the Himalayan foreland basin, NW Himalaya, India: *Journal of Asian Earth Sciences*, v. 23, p. 407–426, [https://doi.org/10.1016/S1367-9120\(03\)00176-7](https://doi.org/10.1016/S1367-9120(03)00176-7).
- La Roche, R.S., Godin, L., Cottle, J.M., and Kellett, D.A., 2016, Direct shear fabric dating constrains early Oligocene onset of the South Tibetan detachment in the western Nepal Himalaya: *Geology*, v. 44, p. 403–406, <https://doi.org/10.1130/G37754.1>.
- Larson, K.P., Ambrose, T.K., Webb, A.A.G., Cottle, J.M., and Shrestha, S., 2015, Reconciling Himalayan midcrustal discontinuities: The Main Central thrust system: *Earth and Planetary Science Letters*, v. 429, p. 139–146, <https://doi.org/10.1016/j.epsl.2015.07.070>.
- Lavé, J., and Avouac, J.P., 2000, Active folding of fluvial terraces across the Siwaliks Hills, Himalayas of central Nepal: *Journal of Geophysical Research: Solid Earth*, v. 105, B3, p. 5735–5770.
- Le Fort, P., 1975, Himalayas: The collided range, present knowledge of the continental arc: *American Journal of Science*, v. 275A, p. 1–44.
- Li, Y., Wang, C., Dai, J., Xu, G., Hou, Y., and Li, X., 2015, Propagation of the deformation and growth of the Tibetan–Himalayan orogen: A review: *Earth-Science Reviews*, v. 143, p. 36–61, <https://doi.org/10.1016/j.earscirev.2015.01.001>.
- Long, S., McQuarrie, N., Tobgay, T., and Grujic, D., 2011, Geometry and crustal shortening of the Himalayan fold-thrust belt, eastern and central Bhutan: *Geological Society of America Bulletin*, v. 123, p. 1427–1447, <https://doi.org/10.1130/B30203.1>.
- Mandal, S., Robinson, D.M., Khanal, S., and Das, O., 2015, Redefining the tectonostratigraphic and structural architecture of the Almora klippe and Ramgarh–Munsiari thrust in north-west India, in *Mukherjee, S., Carosi, R., van der Beek, P.A., Mukherjee, B.K., and Robinson, D.M., eds., Tectonics of the Himalaya: Geological Society [London] Special Publication 412*, p. 247–269, <https://doi.org/10.1144/SP412.6>.
- Mandal, S., Robinson, D.M., Kohn, M.J., Khanal, S., Das, O., and Bose, S., 2016, Zircon U-Pb ages and Hf isotopes of the Askot klippe, Kumaun, northwest India: Implications for Paleoproterozoic tectonics, basin evolution and associated metallogeny of the northern Indian cratonic margin: *Tectonics*, v. 35, p. 965–982, <https://doi.org/10.1002/2015TC004064>.
- Martin, A.J., 2016, A review of definitions of the Himalayan Main Central thrust: *International Journal of Earth Sciences*, v. 106, no. 6, p. 2131–2145.
- Martin, A.J., 2017, A review of Himalayan stratigraphy, magmatism, and structure: *Gondwana Research*, v. 49, p. 42–80, <https://doi.org/10.1016/j.gr.2017.04.031>.
- Martin, A.J., DeCelles, P.G., Gehrels, G.E., Patchett, P.J., and Isachsen, C., 2005, Isotopic and structural constraints on the location of the Main Central thrust in the Annapurna Range, central Nepal Himalaya: *Geological Society of America Bulletin*, v. 117, p. 926–944, <https://doi.org/10.1130/B25646.1>.
- Martin, A.J., Burg, K.D., Kaufman, A.J., and Gehrels, G.E., 2011, Stratigraphic and tectonic implications of field and isotopic constraints on depositional ages of Proterozoic Lesser Himalayan rocks in central Nepal: *Precambrian Research*, v. 185, p. 1–17, <https://doi.org/10.1016/j.precamres.2010.11.003>.
- McKenzie, N.R., Hughes, N.C., Myrow, P.M., Xiao, S., and Sharma, M., 2011, Correlation of Precambrian–Cambrian sedimentary successions across northern India and the utility of isotopic signatures of Himalayan lithotectonic zones: *Earth and Planetary Science Letters*, v. 312, p. 471–483, <https://doi.org/10.1016/j.epsl.2011.10.027>.
- McQuarrie, N., and Ehlers, T.A., 2015, Influence of thrust belt geometry and shortening rate on thermochronometer cooling ages: Insights from thermokinematic and erosion modeling of the Bhutan Himalaya: *Tectonics*, v. 34, p. 1055–1079, <https://doi.org/10.1002/2014TC003783>.
- McQuarrie, N., and Ehlers, T.A., 2017, Techniques for understanding fold-thrust belt kinematics and thermal evolution, in *Law, R.D., Thigpen, J.R., Merschat, A.J., and Stowell, H.H., eds., Linkages and Feedbacks in Orogenic Systems: Geological Society of America Memoir 213*, p. 25–54, [https://doi.org/10.1130/2017.1213\(02\)](https://doi.org/10.1130/2017.1213(02)).

- McQuarrie, N., Robinson, D., Long, S., Tobgay, T., Grujic, D., Gehrels, G., and Ducea, M., 2008, Preliminary stratigraphic and structural architecture of Bhutan: Implications for the along strike architecture of the Himalayan system: *Earth and Planetary Science Letters*, v. 272, p. 105–117, <https://doi.org/10.1016/j.epsl.2008.04.030>.
- McQuarrie, N., Tobgay, T., Long, S.P., Reiners, P.W., and Cosca, M.A., 2014, Variable exhumation rates and variable displacement rates: Documenting recent slowing of Himalayan shortening in western Bhutan: *Earth and Planetary Science Letters*, v. 386, p. 161–174, <https://doi.org/10.1016/j.epsl.2013.10.045>.
- Miller, C., Klötzli, U., Frank, W., Thöni, M., and Grasemann, B., 2000, Proterozoic crustal evolution in the NW Himalaya (India) as recorded by circa 1.80 Ga mafic and 1.84 Ga granitic magmatism: *Precambrian Research*, v. 103, no. 3–4, p. 191–206.
- Mishra, P., and Mukhopadhyay, D.K., 2012, Structural evolution of the frontal fold-thrust belt, NW Himalayas, from sequential restoration of balanced cross-sections and its hydrocarbon potential, in Bhat, G.M., Craig, J., Thurow, J.W., Thusu, B., and Cozzi, A., eds., *Geology and Hydrocarbon Potential of Neoproterozoic–Cambrian Basins in Asia*: Geological Society [London] Special Publication 366, p. 201–228, <https://doi.org/10.1144/SP366.6>.
- Mitra, G., Bhattacharyya, K., and Mukul, M., 2010, The Lesser Himalayan duplex in Sikkim: Implications for variations in Himalayan shortening: *Journal of the Geological Society of India*, v. 75, no. 1, p. 289–301.
- Mondal, M.E.A., Goswami, J.N., Deomurari, M.P., and Sharma, K.K., 2002, Ion microprobe $^{207}\text{Pb}/^{206}\text{Pb}$ ages of zircons from the Bundelkhand massif, northern India: implications for crustal evolution of the Bundelkhand–Aravalli protocontinent: *Precambrian Research*, v. 117, no. 1–2, p. 85–100.
- Montemagni, C., Iaccarino, S., Montomoli, C., Carosi, R., Jain, A.K., and Villa, I.M., 2018, Age constraints on the deformation style of the South Tibetan detachment system in Garhwal Himalaya: *Italian Journal of Geosciences*, v. 137, p. 175–187, <https://doi.org/10.3301/IJG.2018.07>.
- Montemagni, C., Montomoli, C., Iaccarino, S., Carosi, R., Jain, A.K., Massonne, H.J., and Villa, I.M., 2019, Dating protracted fault activities: Microstructures, microchemistry and geochronology of the Vaikrita thrust, Main Central thrust zone, Garhwal Himalaya, NW India, in Sharma, R., Villa, I.M., and Kumar, S., eds., *Crustal Architecture and Evolution of the Himalaya–Karakoram–Tibet Orogen*: Geological Society [London] Special Publication 481 (in press), <https://doi.org/10.1144/SP481.3>.
- Montomoli, C., Iaccarino, S., Carosi, S., Langone, A., and Visonà, D., 2013, Tectonometamorphic discontinuities within the Greater Himalayan Sequence in western Nepal (Central Himalaya): Insights on the exhumation of crystalline rocks: *Tectonophysics*, v. 26, p. 478–489, <https://doi.org/10.1016/j.tecto.2013.06.006>.
- Montomoli, C., Carosi, R., and Iaccarino, S., 2015, Tectonometamorphic discontinuities in the Greater Himalayan Sequence: A local or a regional feature?, in Mukherjee, S., Carosi, R., van der Beek, P.A., Mukherjee, B.K., and Robinson, D.M., eds., *Tectonics of the Himalaya*: Geological Society [London] Special Publication 412, p. 25–41, <https://doi.org/10.1144/SP412.3>.
- Montomoli, C., Iaccarino, S., Antolin, B., Appel, E., Carosi, R., Dunkl, I., Lin, D., and Visonà, D., 2017, Tectono-metamorphic evolution of the Tethyan Sedimentary Sequence (Himalayas, SE Tibet): *Italian Journal of Geosciences*, v. 136, p. 73–88, <https://doi.org/10.3301/IJG.2015.42>.
- Mukhopadhyay, D.K., and Mishra, P., 2005, A balanced cross section across the Himalayan frontal fold-thrust belt, Subathu area, Himachal Pradesh, India: Thrust sequence, structural evolution and shortening: *Journal of Asian Earth Sciences*, v. 25, p. 735–746, <https://doi.org/10.1016/j.jseae.2004.07.007>.
- Murphy, M.A., and Yin, A., 2003, Structural evolution and sequence of thrusting in the Tethyan fold-thrust belt and Indus-Yalu suture zone, southwest Tibet: *Geological Society of America Bulletin*, v. 115, p. 21–34, [https://doi.org/10.1130/0016-7606\(2003\)115<0021:SEASOT>2.0.CO;2](https://doi.org/10.1130/0016-7606(2003)115<0021:SEASOT>2.0.CO;2).
- Myrow, P.M., Hughes, N.C., Paulsen, T.S., Williams, I.S., Parcha, S.K., Thompson, K.R., Bowring, S.A., Peng, S.-C., and Ahluwalia, A.D., 2003, Integrated tectonostratigraphic reconstruction of the Himalaya and implications for its tectonic reconstruction: *Earth and Planetary Science Letters*, v. 212, p. 433–441, [https://doi.org/10.1016/S0012-821X\(03\)00280-2](https://doi.org/10.1016/S0012-821X(03)00280-2).
- Myrow, P.M., Hughes, N.C., Gooch, J.W., Fanning, C.M., Williams, I.S., Peng, S., Bhargava, O.N., Parcha, S.K., and Pogue, K.R., 2010, Extraordinary transport and mixing of sediment across Himalayan central Gondwana during the Cambrian–Ordovician: *Geological Society of America Bulletin*, v. 122, p. 1660–1670, <https://doi.org/10.1130/B30123.1>.
- Myrow, P.M., Hughes, N.C., Derry, L.A., McKenzie, N.R., Jiang, G., Webb, A.A.G., Banerjee, D.M., Paulsen, T.S., and Singh, B.P., 2015, Neogene marine isotopic evolution and the erosion of Lesser Himalayan strata: Implications for Cenozoic tectonic history: *Earth and Planetary Science Letters*, v. 417, p. 142–150, <https://doi.org/10.1016/j.epsl.2015.02.016>.
- Najman, Y., 2006, The detrital record of orogenesis: A review of approaches and techniques used in the Himalayan sedimentary basins: *Earth-Science Reviews*, v. 74, p. 1–72, <https://doi.org/10.1016/j.earscirev.2005.04.004>.
- Najman, Y., Bickle, M., BouDagher-Fadel, M., Carter, A., Garzanti, E., Paul, M., Wijbrans, J., Willett, E., Oliver, G., Parrish, R., and Akhter, S.H., 2008, The Paleogene record of Himalayan erosion: Bengal Basin, Bangladesh: *Earth and Planetary Science Letters*, v. 273, no. 1–2, p. 1–14.
- Najman, Y., Appel, E., Boudagher-Fadel, M., Bown, P., Carter, A., Garzanti, E., Godin, L., Han, J., Liebke, U., Oliver, G., Parrish, R., and Vezzoli, G., 2010, Timing of India-Asia collision: Geological, biostratigraphic, and palaeomagnetic constraints: *Journal of Geophysical Research*, v. 115, B12416, <https://doi.org/10.1029/2010JB007673>.
- Ojha, T.P., Butler, R.F., DeCelles, P.G., and Quade, J., 2009, Magnetic polarity stratigraphy of the Neogene foreland basin deposits of Nepal: *Basin Research*, v. 21, no. 1, p. 61–90.
- Parkash, B., Sharma, R., and Roy, A.K., 1980, The Siwalik Group (molasses)—Sediments shed by collision of continental plates: *Sedimentary Geology*, v. 25, p. 127–159, [https://doi.org/10.1016/0037-0738\(80\)90058-5](https://doi.org/10.1016/0037-0738(80)90058-5).
- Parrish, R.R., and Hodges, K.V., 1996, Isotopic constraints on the age and provenance of the Lesser and Greater Himalayan Sequences, Nepalese Himalaya: *Geological Society of America Bulletin*, v. 108, p. 904–911, [https://doi.org/10.1130/0016-7606\(1996\)108<0904:ICOTAA>2.3.CO;2](https://doi.org/10.1130/0016-7606(1996)108<0904:ICOTAA>2.3.CO;2).
- Parsons, A.J., Phillips, R.J., Lloyd, G.E., Law, R.D., Searle, M.P., and Walshaw, R.D., 2016, Mid-crustal deformation of the Annapurna-Dhaulagiri Himalaya, central Nepal: An atypical example of channel flow during the Himalayan orogeny: *Geosphere*, v. 12, p. 985–1015, <https://doi.org/10.1130/GES01246.1>.
- Parui, C., and Bhattacharyya, K., 2018, Duplex and along-strike structural variation: A case study from Sikkim Himalayan fold thrust belt: *Journal of Structural Geology*, v. 113, p. 62–75, <https://doi.org/10.1016/j.jsg.2018.05.017>.
- Patchett, P.J., and Ruiz, J., 1987, Nd isotopic ages of crust formation and metamorphism in the Precambrian of eastern and southern Mexico: *Contributions to Mineralogy and Petrology*, v. 96, no. 4, p. 523–528.
- Patel, R.C., Kumar, Y., Lal, N., and Kumar, A., 2007, Thermotectonic history of the Chiplakot Crystalline Belt in the Lesser Himalaya, Kumaon, India: Constraints from apatite fission-track thermochronology: *Journal of Asian Earth Sciences*, v. 29, p. 430–439, <https://doi.org/10.1016/j.jseae.2006.04.008>.
- Patel, R.C., Adlaka, V., Singh, P., Kumar, J., and Lal, N., 2011, Geology, structural and exhumation history of the Higher Himalayan Crystalline in Kumaon Himalaya, India: *Journal of the Geological Society of India*, v. 77, p. 47–72, <https://doi.org/10.1007/s12594-011-0008-5>.
- Patel, R.C., Singh, P., and Lal, N., 2015, Thrusting and back-thrusting as post-emplacment kinematics of the Almora klippe: Insights from low-temperature thermochronology: *Tectonophysics*, v. 653, p. 41–51, <https://doi.org/10.1016/j.tecto.2015.03.025>.
- Peyton, S.L., and Carrapa, B., 2013, An introduction to low-temperature thermochronologic techniques, methodology, and applications, in Knight, C., and Czuzela, J., eds., *Application of Structural Methods to Rocky Mountain Hydrocarbon Exploration and Development*: American Association of Petroleum Geology Studies in Geology 65, p. 15–36.
- Phukon, P., Sen, K., Srivastava, H.B., Singhal, S., and Sen, A., 2018, U-Pb geochronology and geochemistry from the Kumaun Himalaya, NW India, reveal Paleoproterozoic arc magmatism related to formation of the Columbia supercontinent: *Geological Society of America Bulletin*, v. 130, no. 7–8, p. 1164–1176, <https://doi.org/10.1130/B31866.1>.
- Raiverman, V., 2002, Foreland Sedimentation in Himalayan Tectonic Regime: A Relook at the Orogenic Process: Dehradun, India, Bishen Singh Mahendra Pal Singh, 278 p.
- Ravikant, V., Wu, F.Y., and Ji, W.Q., 2011, U-Pb age and Hf isotopic constraints of detrital zircons from the Himalayan foreland Subathu sub-basin on the Tertiary palaeogeography of the Himalaya: *Earth and Planetary Science Letters*, v. 304, p. 356–368, <https://doi.org/10.1016/j.epsl.2011.02.009>.
- Rawat, R., and Sharma, R., 2011, Features and characterization of graphite in Almora Crystal-lines and their implication for the graphite formation in Lesser Himalaya, India: *Journal of Asian Earth Sciences*, v. 42, no. 1–2, p. 51–64.
- Richards, A., Argles, T., Harris, N., Parrish, R., Ahmad, T., Darbyshire, F., and Draganits, E., 2005, Himalayan architecture constrained by isotopic tracers from clastic sediments: *Earth and Planetary Science Letters*, v. 236, p. 773–796, <https://doi.org/10.1016/j.epsl.2005.05.034>.
- Robinson, D.M., 2008, Forward modeling the kinematic sequence of the central Himalayan thrust belt, western Nepal: *Geosphere*, v. 4, p. 785–801, <https://doi.org/10.1130/GES00163.1>.
- Robinson, D.M., and Martin, A.J., 2014, Reconstructing the Greater Indian margin: A balanced cross section in central Nepal focusing on the Lesser Himalayan duplex: *Tectonics*, v. 33, p. 2143–2168, <https://doi.org/10.1002/2014TC003564>.
- Robinson, D.M., and McQuarrie, N., 2012, Pulsed deformation and variable slip rates within the central Himalayan thrust belt: *Lithosphere*, v. 4, p. 449–464, <https://doi.org/10.1130/L204.1>.
- Robinson, D.M., and Pearson, O.N., 2013, Was Himalayan normal faulting triggered by initiation of the Ramgarh-Munsiari thrust and development of the Lesser Himalayan duplex?: *International Journal of Earth Sciences*, v. 102, p. 1773–1790, <https://doi.org/10.1007/s00531-013-0895-3>.
- Robinson, D.M., DeCelles, P.G., Patchett, P.J., and Garzzone, C.N., 2001, The kinematic evolution of the Nepalese Himalaya interpreted from Nd isotopes: *Earth and Planetary Science Letters*, v. 192, p. 507–521, [https://doi.org/10.1016/S0012-821X\(01\)00451-4](https://doi.org/10.1016/S0012-821X(01)00451-4).
- Robinson, D.M., DeCelles, P.G., Garzzone, C.N., Pearson, O.N., Harrison, T.M., and Catlos, E.J., 2003, Kinematic model for the Main Central thrust in Nepal: *Geology*, v. 31, p. 359–362, [https://doi.org/10.1130/0091-7613\(2003\)031<0359:KMFTMC>2.0.CO;2](https://doi.org/10.1130/0091-7613(2003)031<0359:KMFTMC>2.0.CO;2).
- Robinson, D.M., DeCelles, P.G., and Copeland, P., 2006, Tectonic evolution of the Himalayan thrust belt in western Nepal: Implications for channel flow models: *Geological Society of America Bulletin*, v. 118, p. 865–885, <https://doi.org/10.1130/B25911.1>.
- Rupke, J., 1974, Stratigraphic and structural evolution of the Kumaun Lesser Himalaya: *Sedimentary Geology*, v. 11, p. 81–265, [https://doi.org/10.1016/0037-0738\(74\)90027-X](https://doi.org/10.1016/0037-0738(74)90027-X).
- Sachan, H.K., Kohn, M.J., Saxena, A., and Corrie, S.L., 2010, The Malari leucogranite, Garhwal Himalaya, northern India: Chemistry, age, and tectonic implications: *Geological Society of America Bulletin*, v. 122, p. 1865–1876, <https://doi.org/10.1130/B30153.1>.
- Sastri, S., Bhandari, L.L., Raju, T.R., and Datta, A.K., 1971, Tectonic framework and subsurface stratigraphy of the Ganga Basin: *Journal of the Geological Society of India*, v. 12, p. 222–233.
- Schelling, D., and Arita, K., 1991, Thrust tectonics, crustal shortening, and the structure of the far-eastern Nepal, Himalaya: *Tectonics*, v. 10, p. 851–862, <https://doi.org/10.1029/91TC01011>.
- Searle, M.P., 1999, Emplacement of Himalayan leucogranites by magma injection along giant sill complexes: examples from the Cho Oyu, Gyachung Kang and Everest leucogranites (Nepal Himalaya): *Journal of Asian Earth Sciences*, v. 17, no. 5–6, p. 773–783.
- Searle, M., Law, R.D., Godin, L., Larson, K., Streule, M.J., Cottle, J.M., and Jessup, M.J., 2008, Defining the Himalayan Main Central thrust in Nepal: *Journal of the Geological Society [London]*, v. 165, p. 523–534, <https://doi.org/10.1144/0016-7642007-081>.
- Searle, M.P., Cottle, J.M., Streule, M.J., and Waters, D.J., 2009, Crustal melt granites and migmatites along the Himalaya: melt source, segregation, transport and granite emplacement

- mechanisms: *Earth and Environmental Science Transactions of the Royal Society of Edinburgh*, v. 100, no. 1-2, p. 219–233.
- Searle, M., Avouac, J.P., Elliott, J., and Dyck, B., 2016, Ductile shearing to brittle thrusting along the Nepal Himalaya: Linking Miocene channel flow and critical wedge tectonics to 25th April 2015 Gorkha earthquake: *Tectonophysics*, v. 714, p. 117–124, <https://doi.org/10.1016/j.tecto.2016.08.003>.
- Sen, K., Chaudhury, R., and Pfänder, J., 2015, $^{40}\text{Ar}/^{39}\text{Ar}$ age constraint on deformation and brittle-ductile transition of the Main Central thrust and the South Tibetan detachment zone from Dhauliganga valley, Garhwal Himalaya, India: *Journal of Geodynamics*, v. 88, p. 1–13, <https://doi.org/10.1016/j.jog.2015.04.004>.
- Shah, J., Srivastava, D.C., and Joshi, S., 2012, Sinistral transpression along the Main Boundary Thrust in Amritpur area, Southeastern Kumaun Himalaya, India: *Tectonophysics*, v. 532, p. 258–270, <https://doi.org/10.1016/j.tecto.2012.02.012>.
- Singh, P., and Patel, R.C., 2017, Post-emplacement kinematics and exhumation history of the Almora klippe of the Kumaun–Garhwal Himalaya, NW India: Revealed by fission track thermochronology: *International Journal of Earth Sciences*, v. 106, p. 2189–2202, <https://doi.org/10.1007/s00531-016-1422-0>.
- Spencer, C.J., Harris, R.A., and Dorais, M.J., 2012a, The metamorphism and exhumation of the Himalayan metamorphic core, eastern Garhwal region, India: *Tectonics*, v. 31, TC1007, <https://doi.org/10.1029/2010TC002853>.
- Spencer, C.J., Harris, R.A., and Dorais, M.J., 2012b, Depositional provenance of the Himalayan metamorphic core of Garhwal region, India: Constrained by U–Pb and Hf isotopes in zircons: *Gondwana Research*, v. 22, p. 26–35, <https://doi.org/10.1016/j.gr.2011.10.004>.
- Srivastava, P., and Mitra, G., 1994, Thrust geometries and deep structure of the outer and Lesser Himalaya, Kumaun and Garhwal (India): Implications for evolution of the Himalayan fold-and-thrust belt: *Tectonics*, v. 13, p. 89–109, <https://doi.org/10.1029/93TC01130>.
- Suppe, J., 1983, Geometry and kinematics of fault-bend folding: *American Journal of Science*, v. 283, p. 684–721, <https://doi.org/10.2475/ajs.283.7.684>.
- Valdiya, K.S., 1980, *Geology of Kumaun Lesser Himalaya: Dehradun, India*, Wadia Institute of Himalayan Geology Publication, 291 p.
- Valdiya, K.S., Paul, S.K., Tarachandra, Bhakuni, S.S., and Upadhyay, R.C., 1999, Tectonic and lithological characterization of Himadri (Great Himalaya) between Kali and Yamuna rivers, Central Himalaya: *Himalayan Geology*, v. 10, no. 2, p. 1–17.
- van Hinsbergen, D.J.J., Kapp, P., Dupont-Nivet, G., Lippert, P.C., DeCelles, P.G., and Torsvik, T.H., 2011, Restoration of Cenozoic deformation in Asia and the size of Greater India: *Tectonics*, v. 30, TC5003, <https://doi.org/10.1029/2011TC002908>.
- van Hinsbergen, D.J., Lippert, P.C., Dupont-Nivet, G., McQuarrie, N., Doubrovine, P.V., Spakman, W., and Torsvik, T.H., 2012, Greater India Basin hypothesis and a two-stage Cenozoic collision between India and Asia: *Proceedings of the National Academy of Sciences*, v. 109, p. 7659–7664, <https://doi.org/10.1073/pnas.1117262109>.
- Vervoort, J.D., and Patchett, P.J., 1996, Behavior of hafnium and neodymium isotopes in the crust: constraints from Precambrian crustally derived granites: *Geochimica et Cosmochimica Acta*, v. 60, no. 19, p. 3717–3733.
- Vervoort, J.D., Patchett, P.J., Söderlund, U., and Baker, M., 2004, Isotopic composition of Yb and the determination of Lu concentrations and Lu/Hf ratios by isotope dilution using MC-ICPMS: *Geochemistry, Geophysics, Geosystems*, v. 5, no. 11, <https://doi.org/10.1029/2004GC000721>.
- Visonà, D., and Lombardo, B., 2002, Two-mica and tourmaline leucogranites from the Everest-Makalu region (Nepal-Tibet). Himalayan leucogranite genesis by isobaric heating: *Lithos*, v. 62, p. 125–150, [https://doi.org/10.1016/S0024-4937\(02\)00112-3](https://doi.org/10.1016/S0024-4937(02)00112-3).
- Wang, J.M., Rubatto, D., and Zhang, J.J., 2015, Timing of partial melting and cooling across the Greater Himalayan Crystalline Complex (Nyalam, central Himalaya): In-sequence thrusting and its implications: *Journal of Petrology*, v. 56, p. 1677–1702, <https://doi.org/10.1093/ptrology/egv050>.
- Webb, A.A.G., 2013, Preliminary balanced palinspastic reconstruction of Cenozoic deformation across the Himachal Himalaya (northwestern India): *Geosphere*, v. 9, p. 572–587, <https://doi.org/10.1130/GES00787.1>.
- Webb, A.A.G., Yin, A., Harrison, T.M., Célérier, J., and Burgess, W., 2007, The leading edge of the Greater Himalayan Crystallines revealed in the NW Indian Himalaya: Implications for the evolution of the Himalayan orogen: *Geology*, v. 35, p. 955–958, <https://doi.org/10.1130/G23931A.1>.
- Webb, A.A.G., Guo, H., Clift, P.D., Husson, L., Müller, T., Costantino, D., Yin, A., Xu, Z., Cao, H., and Wang, Q., 2017, The Himalaya in 3D: Slab dynamics controlled mountain building and monsoon intensification: *Lithosphere*, v. 9, no. 4, p. 637–651, <https://doi.org/10.1130/L636.1>.
- Wesnously, S.G., Kumar, S., Mohindra, R., and Thakur, V.C., 1999, Uplift and convergence along the Himalayan Frontal Thrust of India: *Tectonics*, v. 18, p. 967–976.
- White, N.M., Pringle, M.S., Garzanti, E., Bickle, M.J., Najman, Y.M.R., Chapman, H., and Friend, P., 2002, Constraints on the exhumation and erosion of the High Himalayan slab, NW India, from foreland basin deposits: *Earth and Planetary Science Letters*, v. 195, p. 29–44, [https://doi.org/10.1016/S0012-821X\(01\)00565-9](https://doi.org/10.1016/S0012-821X(01)00565-9).
- Yin, A., 2006, Cenozoic tectonic evolution of the Himalayan orogen as constrained by along-strike variation of structural geometry, exhumation history, and foreland sedimentation: *Earth-Science Reviews*, v. 76, p. 1–131, <https://doi.org/10.1016/j.earscirev.2005.05.004>.
- Yin, A., and Harrison, T.M., 2000, Geologic evolution of the Himalayan-Tibetan orogen: *Annual Review of Earth and Planetary Sciences*, v. 28, p. 211–280.
- Yin, A., Dubey, C.S., Kelty, T.K., Webb, A.A.G., Harrison, T.M., Chou, C.Y., and Célérier, J., 2010, Geologic correlation of the Himalayan orogen and Indian craton: Part 2. Structural geology, geochronology, and tectonic evolution of the Eastern Himalaya: *Geological Society of America Bulletin*, v. 122, p. 360–395, <https://doi.org/10.1130/B26461.1>.
- Yu, H., Webb, A.A.G., and He, D., 2015, Extrusion vs. duplexing models of Himalayan mountain building 1: Discovery of the Pabbar thrust confirms duplex-dominated growth of the northwestern Indian Himalaya since mid-Miocene: *Tectonics*, v. 34, p. 313–333, <https://doi.org/10.1002/2014TC003589>.

MANUSCRIPT RECEIVED 30 OCTOBER 2018

REVISED MANUSCRIPT RECEIVED 25 JANUARY 2019

MANUSCRIPT ACCEPTED 4 MARCH 2019